Polyhedron 62 (2013) 89–103

Contents lists available at SciVerse ScienceDirect

Polyhedron

journal homepage: www.elsevier.com/locate/poly

Rhenium complexes of di-2-pyridyl ketone, 2-benzoylpyridine and 2-hydroxybenzophenone: A structural and theoretical study

N.C. Yumata [a], G. Habarurema [a], J. Mukiza [a], T.I.A. Gerber [a,*], E. Hosten [a], F. Taherkhani [b,*], M. Nahali [c]

[a] Department of Chemistry, Nelson Mandela Metropolitan University, Port Elizabeth, South Africa
[b] Department of Physical Chemistry, Razi University, Kermanshah, Iran
[c] Department of Science, Babol Noshiravani University of Technology, Babol, Iran

ARTICLE INFO

Article history:
Received 7 May 2013
Accepted 16 June 2013
Available online 29 June 2013

Keywords:
Di-2-pyridyl ketone
2-Benzoylpyridine
Reduction
fac-$[Re(CO)_3]^+$
DFT
TD-DFT
NBO

ABSTRACT

The reactions of di-2-pyridyl ketone (dpk), 2-benzoylpyridine (zpy) and 2-hydroxybenzophenone (Hbp) with $[Re(CO)_5Cl]$ (**A**) and *trans*-$[ReOX_3(PPh_3)_2]$ (**B**, X = Cl, Br) were studied. The complex *fac*-$[Re(CO)_3(dpk{\cdot}OCH_3)]$ was isolated from the reaction of **A** with dpk in methanol. The monoanionic tridentate chelate dpk·OCH_3 was formed by the nucleophilic attack of methanol at the carbonylic carbon atom of dpk. A similar attack of water on dpk was observed in the compound *cis*-$[ReOBr_2(dpk{\cdot}OH)]{\cdot}2(dpkH^+Br^-)$, which was formed from dpk and $[ReOBr_3(PPh_3)_2]$ in acetone. The reaction of zpy with **B** in acetonitrile produced the complexes $[Re^{III}X_3(zpy)(PPh_3)]$, but in methanol as solvent the compounds $[ReOX_2(zpyH)(PPh_3)]$ were isolated, where zpyH coordinates bidentately as the monoanionic ligand $[C_6H_5(HC\text{-}O)C_5H_4N]^-$. With **A** as starting material the complex *fac*-$[Re(CO)_3(zpy)Cl]$ was isolated. The complexes *cis*-$[ReOX_2(bp)(PPh_3)]$ were the products of the reaction of Hbp with **B** in acetonitrile; however, in methanol *cis*-$[Re^{III}Br_2(bp)(PPh_3)_2]$ was isolated. All these complexes were characterized by conductance measurements, elemental analyses, UV–Vis, IR and NMR spectroscopy and by single crystal X-ray diffraction. DFT calculations regarding the electronic ground states show single states for all the complexes, except for the rhenium(III) complexes $[Re^{III}X_3(zpy)(PPh_3)]$ and $[ReBr_2(bp)(PPh_3)_2]$, in which the states are triplet. The DFT and experimental results are in agreement in all cases, especially the anisotropy of the Re–N bond length of *fac*-$[Re(CO)_3(dpk{\cdot}OCH_3)]$ and exact O(1)–Re–O(3) angles for $[ReOX_2(bp)(PPh_3)]$.

1. Introduction

The CO-bridged pyridyl derivatives di-2-pyridyl ketone (dpk) and 2-benzoylpyridine (zpy) were shown to have interesting coordination behavior. It was found that dpk and zpy can coordinate to the metal ion in a variety of modes. Dpk can act as a bidentate, tridentate or bridging ligand [1], whereas with zpy, the ligand can either bind monodentately (through the pyridyl nitrogen or carbonylic oxygen atom), as a neutral bidentate or as a bridging chelate to the metal center [2–4]. Elegant work by Machura et al. has shown that dpk coordinates as a bidentate N,O-donor ligand in the complex $[Re^{III}Cl_3(dpk)PPh_3)]$, which on standing in chloroform led to the N,N-chelation of dpk in the rhenium(III) compound $[ReCl_3(dpk)(OPPh_3)]$ [5a]. It was previously reported that dpk undergoes nucleophilic attack by water or alcohols at the carbonylic carbon to give complexes containing dpk·H_2O or dpk·OH (Scheme 1) [1]. Examples of the latter are the oxorhenium(V) complex $[ReOCl_2\{(C_5H_4N)_2C(O)(OH)\}]$ [1a] and $[Re^I(CO)_3(dpk{\cdot}OH)]$ [1b], in which the chelate acts as a uninegative tridentate ligand.

Interest in the metal-promoted nucleophilic attack of water stems from the fact that ketones do not normally hydrate to a significant degree in the absence of strong electron-withdrawing groups [5]. It was shown that the oxidation state of the metal determines to a large degree the coordination mode of ligands with a ketone group. Nucleophilic attack by water/alcohol on these ligands is promoted by electron-deficient high oxidation state oxorhenium(V) centers, whereas the coordination through the pyridyl nitrogen and neutral carbonyl oxygen is observed in rhenium(I) and (III) complexes [5].

In this account the study of the reactions of di-2-pyridyl ketone (dpk), 2-benzoylpyridine (zpy), and also 2-hydroxybenzophenone (Hbp), with the $[ReO]^{3+}$ and $[Re(CO)_3]^+$ moieties are reported. In a previous reaction of $[Re(CO)_3(dpk)Cl]$ with an ethanol/water mixture, only the derivative $[Re(CO)_3(dpk{\cdot}OH)]$, and not $[Re(CO)_3(dpk{\cdot}OEt)]$, was isolated [6]. In this study we have reacted $[Re(CO)_5Cl]$ with dpk in methanol to produce *fac*-$[Re(CO)_3(dpk{\cdot}OCH_3)]$. Our study was extended to also include the possible nucleophilic attack on the carbonylic carbon atom of the related compound 2-benzoylpyridine, which, when reacted with [ReOX$_3$

---

* Corresponding authors. Tel.: +27 425044285 (T.I.A. Gerber).
E-mail addresses: thomas.gerber@nmmu.ac.za (T.I.A. Gerber), f.taherkani@razi.ac.ir (F. Taherkhani).

0277-5387/$ - see front matter © 2013 Elsevier Ltd. All rights reserved.
http://dx.doi.org/10.1016/j.poly.2013.06.025

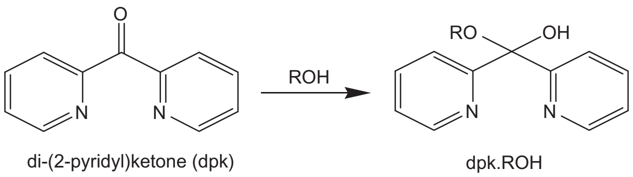

Scheme 1. Nucleophilic attack of ROH at the carbonylic carbon atom.

$(PPh_3)_2]$ (X = Cl, Br), produced the species $[Re^{III}X_3(zpy)(PPh_3)]$ in acetonitrile but $[ReOX_2(zpyH)(PPh_3)]$ in methanol. In the latter reaction the coordinated zpy ligand has been reduced to the phenyl-2-pyridylmethanolate anion [zpyH$^-$, $\{C_6H_5(HC\text{-}O)C_5H_4N\}^-$)]. These results are similar to those reported by Machura et al., albeit under different experimental conditions [7]. We have also studied the coordination behavior of the related ligand 2-hydroxybenzophenone, which on reaction with $[ReOX_3(PPh_3)_2]$ in methanol and acetonitrile gave the products $[Re^{III}X_2(bp)(PPh_3)_2]$ and $[Re^{V}OX_2(bp)(PPh_3)]$ respectively, with no nucleophilic attack on the carbonylic carbon of bp$^-$ being observed.

2. Experimental

2.1. Materials and instrumentation

All materials were commercially available and used as received. *trans*-$[ReOX_3(PPh_3)_2]$ (X = Cl, Br) was prepared by a literature method [8], and $[Re(CO)_5Cl]$ and the ligands di-2-pyridyl ketone (dpk), 2-benzoylpyridine (zpy) and 2-hydroxybenzophenone (Hbp) were obtained from Aldrich.

Infrared (IR) spectra were recorded on a Digilab FTS3100 Excalibur HE spectrophotometer and were run as KBr pellets. ^{1}H NMR spectra were recorded on a Bruker Avance 300 MHz spectrometer as solutions in DMSO-d_6 at 25 °C, using TMS as internal standard. Electronic spectra were obtained with a Shimadzu UV-3100 spectrophotometer. Microanalyses were obtained on a Carlo Erba EA1108 elemental analyser, and melting points were determined on an Electrothermal IA-900 apparatus. Conductivity measurements (in the unit $ohm^{-1}\,cm^2\,mol^{-1}$) were carried out with 10^{-3} M solutions at 298 K with a Phillips PW9509 conductometer.

2.2. Syntheses of the complexes

2.2.1. fac-[Re(CO)$_3$(dpk·OCH$_3$)] (**1**)

A mixture of dpk (109 mg, 592 μmol) and $[Re(CO)_5Cl]$ (107 mg, 296 μmol) was heated at reflux in 20 cm^3 of methanol for 2 h under nitrogen. The resultant yellow solution was cooled to room temperature and the precipitate which formed was filtered, washed with diethyl ether and dried under vacuum. Orange crystals were obtained by the slow evaporation of the mother liquor. Yield = 73%, m.p. 278 °C. *Anal.* Calc. for $C_{15}H_{11}N_2O_5Re$: C, 37.1; H, 2.3; N, 5.8. Found: C, 37.3; H, 2.1; N, 5.9%. IR (cm^{-1}): $\nu(C{=}O)_{fac}$ 2007vs, 1914vs, 1857vs; ν(C=N) 1585m; ν(C=C) 1540m, 1463m; ν(Re–N) 484m, 430m. ^{1}H NMR (DMSO-d_6, ppm): 9.23 (d, 2H, *H15*, *H25*); 8.42 (t, 2H, *H13*, *H23*); 8.21 (d, 2H, *H12*, *H22*); 8.13 (t, 2H, *H14*, *H24*); 3.48 (s, 3H, O*CH$_3$*). UV–Vis (dichloromethane, λ_{max} (ε, M^{-1} cm^{-1})): 318 (2260); 377 (540). Conductivity (MeOH): 95.

2.2.2. cis-[ReOBr$_2$(dpk·OH)]·2(dpkH$^+$Br$^-$) (**2**)

To a 102 mg (106 μmol) suspension of *trans*-$[ReOBr_3(PPh_3)_2]$ in 5 cm^3 of acetone was added 381 mg (207 μmol) of dpk dissolved in 10 cm^3 of acetone. The reaction mixture was heated under reflux for 8 h, cooled to room temperature, and a blue precipitate was removed by filtration and dried under vacuum. The mother liquor was left to evaporate slowly at room temperature. After 2 days dark blue crystals, suitable for X-ray diffraction studies, were collected by filtration. Yield = 62%, m.p. 295 °C. *Anal.* Calc. for $C_{33}H_{27}Br_4N_6O_5Re$: C, 36.2; H, 2.5; N, 7.7. Found: C, 36.4; H, 2.3; N, 7.8%. IR (cm^{-1}): υ(C=O) 1693s; υ(C=N) 1605m, 1587m; υ(C=C) 1520s; υ(Re=O) 950s; ν(Re–N) 470s, 465s. ^{1}H NMR (DMSO-d_6, ppm): 8.71–7.67 (Ar *H*). Conductivity (acetone): 122.

2.2.3. [ReX$_3$(zpy)(PPh$_3$)] (X = Cl(**3**), Br(**4**))

A mixture of *trans*-$[ReOX_3(PPh_3)_2]$ (120 μmol) and 240 μmol (440 mg) of zpy in 20 cm^3 of acetonitrile was heated under reflux for 3 h. The resultant blue solution was cooled to room temperature and the precipitate which formed was filtered, washed with diethyl ether and dried under vacuum. Blue crystals were obtained by the slow evaporation of the mother liquor.

*(**3**):* Yield = 65%, m.p. 265 °C. *Anal.* Calc. for $C_{30}H_{24}Cl_3NOPRe$: C, 48.8; H, 3.3; N, 1.9. Found: C, 48.3; H, 3.3; N, 2.1%. IR (cm^{-1}): υ(C=O) 1590 m; υ(C=N) 1605 m, 1587 m; υ(C=C) 1520s; υ(Re–N) 499m; ν(Re–O) 424m; ν(Re–Cl) 324m. ^{1}H NMR (DMSO-d_6, ppm): 8.73 (d, 1H, *H25*); 8.62 (t, 1H, *H23*); 8.45 (d, 1H, *H22*); 8.09 (t, 1H, *H24*); 8.59–7.79 (m, 4H, *H12*, *H13*, *H14*, *H16*); 7.62–7.59 (16H, *H15*, *PPh$_3$*). UV–Vis (CH$_2$Cl$_2$, λ_{max} (ε, M^{-1} cm^{-1})): 318 (19800); 428 (3960); 597(9320). Conductivity (acetone): 125.

*(**4**):* Yield = 68%, m.p. 268 °C. *Anal.* Calc. $C_{30}H_{24}Br_3NOPRe$: C, 41.3; H, 2.8; N, 1.6. Found: C, 41.3; H, 2.7; N, 1.8%. IR (cm^{-1}): υ(C=O) 1589m; υ(C=N) 1605m, 1587m; υ(C=C) 1520s; υ(Re–N) 495m; ν(Re–O) 427m. ^{1}H NMR (DMSO-d_6, ppm): 8.73 (d, 1H, *H15*); 8.62 (t, 1H, *H13*); 8.45 (d, 1H, *H12*); 8.09 (t, 1H, *H14*); 8.59–7.79 (m, 4H, *H22*, *H23*, *H24*, *H26*); 7.62–7.59 (16H, *H25*, *PPh$_3$*). UV–Vis (CH$_2$Cl$_2$, λ_{max} (ε, M^{-1} cm^{-1})): 321 (10940); 468 (2200); 611(4960). Conductivity (acetonitrile): 128.

2.2.4. [ReOX$_2$(zpyH)(PPh$_3$)] (X = Cl(**5**), Br(**6**))

To a suspension of 120 μmol of *trans*-$[ReOX_3(PPh_3)_2]$ in 20 cm^3 of methanol was added 240 μmol of zpy. After the mixture was heated under reflux for 4 h, it was cooled to room temperature and a brown precipitate was collected by filtration.

*(**5**):* Yield = 73%, m.p. 259 °C. *Anal.* Calc. for $C_{30}H_{25}Cl_2NO_2PRe$: C, 50.1; H, 3.5; N, 1.9. Found: C, 50.0; H, 3.3; N, 1.8%. IR (cm^{-1}): υ(Re=O) 948s; ν(Re–N) 473s, 468s; ν(Re–O) 428m; ν(Re–Cl) 329m, 318m. ^{1}H NMR (DMSO-d_6, ppm): 9.21 (s, 1H, *H1*); 8.71 (d, 1H, *H15*); 8.62 (t, 1H, *H13*); 8.45 (d, 1H, *H12*); 8.09 (t, 1H, *H14*); 8.69–7.74 (m, 4H, *H22*, *H23*, *H24*, *H26*); 7.69–7.23 (16H, *H25*; *PPh$_3$*). UV–Vis (CH$_2$Cl$_2$, λ_{max} (ε, M^{-1} cm^{-1})): 345 (7280). Conductivity (acetone): 112.

(**6**): Yield = 69%, m.p. 265 °C. *Anal.* Calc. for $C_{30}H_{25}Br_2NO_2PRe$: C, 44.6; H, 3.1; N, 1.7. Found: C, 44.4; H, 2.9; N, 1.7%. IR (cm^{-1}): υ(Re=O) 944s; ν(Re–N) 470s, 465s; ν(Re-Br) 306m, 298m. ^{1}H NMR (DMSO-d_6, ppm): 9.21 (s, 1H, O*H*); 8.74 (d, 1H, *H15*); 8.64 (t, 1H, *H13*); 8.31 (d, 1H, *H12*); 8.19 (t, 1H, *H14*); 8.59–7.79 (m, 4H, *H22*, *H23*, *H24*, *H26*); 7.71–7.45 (15H, *PPh$_3$*). UV–Vis (CH$_2$Cl$_2$, λ_{max} (ε, M^{-1} cm^{-1})): 365 (7520). Conductivity (acetone): 118.

2.2.5. fac-[Re(CO)$_3$Cl(zpy)].toluene (**7**)

A mixture of zpy (107 mg, 545 μmol) and $[Re(CO)_5Cl]$ (103 mg, 277 μmol) was refluxed in 20 cm^3 of toluene for 4 h under nitrogen. The crystalline maroon precipitate separated upon cooling, and was removed by filtration. Maroon crystals were obtained by the slow evaporation of the mother liquor. Yield = 73%, m.p. 242 °C. *Anal.* Calc. for $C_{15}H_9ClNO_4Re\cdot C_7H_8$: C, 42.1; H, 2.6; N, 2.6. Found: C, 42.0; H, 2.8; N, 2.4%. IR (cm^{-1}): $\nu(C{=}O)_{fac}$ 2021vs, 1916vs, 1857s; ν(C=N) 1571m; ν(C=C) 1550m; ν(Re–N) 460m; ν(Re–Cl) 316m. ^{1}H NMR (DMSO-d_6, ppm): 8.72 (d, 1H, *H15*); 8.08 (t, 1H, *H13*); 7.91–8.01(m, 3H, *H12, H14, H24*); 7.73 (t, 2H, *H22, H26*); 7.65 (t, 2H, *H23, H25*). UV–Vis (dichloromethane, λ_{max} (ε, M^{-1} cm^{-1})): 475 (6820). Conductivity (methanol): 85.

Table 1
Crystal and structure refinement data for complexes **1** to **10**.

	1	**2**	**3**	**4**	**5**	**6**	**7**	**8**	**9**	**10**
Formula weight	485.47	1093.4	738.03	871.38	719.59	808.49	534.95	1067.8	732.58	821.48
Crystal system	triclinic	triclinic	monoclinic	monoclinic	monoclinic	monoclinic	triclinic	orthorhombic	orthorhombic	orthorhombic
Space group	$P\bar{1}$	$P\bar{1}$	$P2_1/c$	$P2_1/c$	$P2_1/c$	$P2_1/c$	$P\bar{1}$	$P2_12_12_1$	$P2_12_12_1$	$P2_12_12_1$
a (Å)	7.820(5)	8.9727(3)	11.6050(2)	11.6368(3)	17.2854(5)	17.6053(4)	7.875(5)	12.6306(3)	9.3659(1)	9.3959(2)
b (Å)	9.052(5)	13.0202(4)	15.2606(2)	15.3684(4)	8.7393(3)	8.8682(2)	9.756(5)	18.1969(5)	15.2231(2)	15.3556(3)
c (Å)	12.477(5)	16.2048(5)	19.2831(2)	19.3340(4)	20.3956(7)	20.5226(4)	12.185(5)	18.8268(6)	19.2618(3)	19.5802(4)
α (°)	106.525(5)	68.707(1)					77.077(5)			
β (°)	95.753(5)	81.943(1)	127.001(1)	125.273(1)	118.534(2)	119.997(1)	83.389(5)			
γ (°)	111.924(5)	79.495(1)					89.240(5)			
Volume (Å^3)	764.0(7)	1728.7(1)	2727.3(7)	2822.9(1)	2706.77(2)	2774.95(1)	906.3(8)	4327.1(2)	2727.32(7)	2825.03(1)
Z	2	2	4	4	4	4	2	4	4	4
D_{calc} (g cm^{-3})	2.11	2.101	1.797	2.05	1.766	1.935	1.96	1.639	1.772	1.931
μ (mm^{-1})	7.979	8.188	4.833	8.633	4.775	7.345	6.874	4.767	4.71	7.218
$F(000)$	460	1044	1440	1656	1408	1552	510	2096	1432	1576
θ range (°)	2.6–28.4	2.5–28.3	2.6–28.3	1.9–28.3	2.6–28.4	2.5–32.3	2.1–28.3	2.2–28.3	2.1–28.3	2.1–28.3
Index ranges	$-10 \leqslant h \leqslant 10$	$-11 \leqslant h \leqslant 11$	$-15 \leqslant h \leqslant 13$	$-15 \leqslant h \leqslant 15$	$-20 \leqslant h \leqslant 23$	$-24 \leqslant h \leqslant 26$	$-10 \leqslant h \leqslant 10$	$-16 \leqslant h \leqslant 15$	$-7 \leqslant h \leqslant 12$	$-12 \leqslant h \leqslant 12$
	$-12 \leqslant k \leqslant 12$	$-17 \leqslant k \leqslant 17$	$-20 \leqslant k \leqslant 20$	$-20 \leqslant k \leqslant 18$	$-11 \leqslant k \leqslant 11$	$-13 \leqslant k \leqslant 13$	$-12 \leqslant k \leqslant 13$	$-24 \leqslant k \leqslant 24$	$-20 \leqslant k \leqslant 20$	$-20 \leqslant k \leqslant 19$
	$-16 \leqslant \ell \leqslant 15$	$-21 \leqslant \ell \leqslant 21$	$-20 \leqslant \ell \leqslant 24$	$-25 \leqslant \ell \leqslant 25$	$-27 \leqslant \ell \leqslant 20$	$-30 \leqslant \ell \leqslant 30$	$-16 \leqslant \ell \leqslant 16$	$-25 \leqslant \ell \leqslant 25$	$-25 \leqslant \ell \leqslant 24$	$-26 \leqslant \ell \leqslant 25$
Observed data [$I > 2.0\sigma(I)$]	3765	7914	3792	5661	4579	5986	4478	9717	6441	6610
Parameters	210	444	334	334	4579	334	251	506	343	343
Goodness of fit (GoF) on F^2	1.09	1.15	0.62	1.01	0.96	0.95	1.07	1.02	0.79	1.04
Final R indices: R	0.0164	0.0167	0.0196	0.0256	0.0346	0.0405	0.0235	0.0214	0.0124	0.0162
$wR2$	0.0407	0.0406	0.0336	0.0616	0.0531	0.0692	0.0601	0.0425	0.029	0.0336
R_{int}	0.03	0.02	0.0369	0.038	0.061	0.058	0.029	0.029	0.015	0.02
Peak/hole (e Å^{-3})	1.11/−1.01	0.50/−0.77	0.56/−0.38	1.63/1.20	1.20/−0.80	1.75/−1.02	1.70/−1.45	0.98/−0.38	0.34/−0.32	0.66/−0.44

Chemical formula: **1**: $C_{15}H_{11}N_2O_5Re$; **2**: $C_{11}H_9Br_2N_2O_3Re$,2($C_{11}H_9N_2O$),2(Br); **3**: $C_{30}H_{24}Cl_3NOPRe$; **4**: $C_{30}H_{24}Br_3NOPRe$; **5**: $C_{30}H_{25}C_{l2}NO_2PRe$; **6**: $C_{30}H_{25}Br_2NO_2PRe$; **7**: $C_{15}H_9ClNO_4Re$, 0.5(C_7H_8); **8**: $C_{49}H_{39}Br_2O_2P_2Re$; **9**: $C_{31}H_{24}Cl_2O_3PRe$; **10**: $C_{31}H_{24}Br_2O_3PRe$.

Table 2
Selected bond lengths [Å] and angles (°) for complexes **1** to **10**.

1					
Re–O(1)	2.095(2)		Re–C(30)	1.911(4)	
Re–N(1)	2.178(3)		Re–C(31)	1.915(3)	
Re–N(2)	2.176(3)		Re–C(32)	1.430(3)	
O(1)–C(1)	1.376(3)		O(2)–C(2)	1.430(3)	
O(1)–Re–C(31)	169.5(1)		N(1)–Re–C(30)	171.7(1)	
O(1)–Re–N(1)	74.8(8)		N(1)–Re–N(2)	82.0(9)	
O(1)–Re–N(2)	74.6(8)		N(2)–Re–C(32)	172.3(1)	
C(1)–O(2)–C(2)	114.4(2)		C(11)–C(1)–C(21)	127.1(2)	
O(1)–C(1)–O(2)	114.4(2)		O(1)–C(1)–C(11)	107.4(2)	
O(1)–C(1)–C(21)	108.5(2)		C(11)–C(1)–O(2)	112.5(2)	
2					
Re–O(11)	1.966(1)		Re–O(13)	1.682(2)	
Re–Br(11)	2.482(3)		Re–Br(12)	2.488(3)	
ReN(11)	2.154(2)		Re–N(12)	2.140(2)	
O(11)–C(1)	1.403(2)		O(12)–C(1)	1.368(3)	
O(11)–Re–O(13)	157.0(7)		N(11)–Re–N(12)	84.9(7)	
O(11)–Re–Br(11)	92.4(5)		O(13)–Re–Br(11)	103.7(6)	
O(11)–Re–Br(12)	87.8(8)		O(13)–Re–Br(12)	102.6(6)	
O(11)–Re–N(11)	74.2(7)		O(13)–Re–N(11)	90.0(8)	
O(11)–Re–N(12)	74.4(7)		O(13)–Re–N(12)	87.8(8)	
O(11)–C(1)–C(111)	105.4(2)		O(12)–C(1)–C(111)	110.3(2)	
Br(11)–Re–N(12)	168.0(5)		Br(12)–Re–N(11)	166.6(5)	
N(11)–C(111)–C(1)	110.7(2)		N(12)–C(121)–C(1)	110.8(2)	
Re–N(11)–C(111)	112.7(2)		Re–N(12)–C(121)	113.2(1)	
	3	**4**		**3**	**4**
Re–X(1)	2.337(8)	2.480(3)	Re–O(1)	2.001(2)	2.016(2)
Re–X(2)	2.341(8)	2.481(4)	Re–N(1)	2.062(2)	2.074(3)
Re–X(3)	2.415(1)	2.572(5)	Re–P(1)	2.446(1)	2.446(2)
O(1)–C(2)	1.285(3)		N(1)–C(25)	1.351(4)	
C(1)–O(1)		1.287(4)	C(11)–N(1)		1.382(4)
X(1)–Re–N(1)	167.9(7)	169.4(8)	O(1)–Re–N(1)	75.5(9)	75.6(1)
X(1)–Re–X(2)	95.1(3)	94.4(1)	P(1)–Re–X(1)	92.2(3)	92.8(2)
X(3)–Re–P(1)	177.3(3)	176.1(3)	P(1)–Re–N(1)	90.8(8)	90.4(2)
O(1)–Re–X(2)	172.0(6)	171.3(7)	P(1)–Re–O(1)	93.4(7)	92.1(8)
	5	**6**		**5**	**6**
Re–X(1)	2.412(1)	2.496(5)	Re–X(2)	2.352(1)	2.560(5)
Re–O(1)	1.919(3)	1.920(3)	Re–O(2)	1.700(3)	1.686(3)
Re–P(1)	2.470(1)	2.477(1)	Re–N(1)	2.197(2)	2.140(3)
C(11)–N(1)	1.347(6)	1.351(6)	C(1)–O(1)	1.422(5)	1.417(4)
O(1)–Re–O(2)	162.6(1)	162.5(1)	O(1)–Re–N(1)	74.9(1)	74.7(1)
O(2)–Re–X(1)	96.6(1)	105.3(9)	O(2)–Re–X(2)	105.6(1)	96.2(1)
O(2)–Re–N(1)	89.6(1)	89.8(1)	O(2)–Re–P(1)	87.0(1)	88.4(1)
Cl(2)–Re–N(1)	164.0(1)		X(2)–Re–O(2)	103.4(5)	101.7(9)
P(1)–Re–Cl(1)	176.4(5)		C(21)–C(1)–O(1)	110.0(3)	106.6(3)
Br(1)–Re–N(1)		164.0(1)	P(1)–Re–Br(2)		174.5(2)
7					
Re–Cl(1)	2.464(2)		Re–C(2)	1.913(4)	
Re–O(1)	2.170(3)		Re–C(3)	1.899(4)	
Re–N(1)	2.162(3)		Re–C(4)	1.911(4)	
O(1)–C(1)	1.246(4)		N(1)–C(11)	1.360(4)	
O(1)–Re–C(3)	171.31(1)		Cl(1)–Re–N(1)	82.60(7)	
N(1)–Re–C(4)	170.9(1)		Cl(1)–Re–O(1)	80.69(7)	
Cl(1)–Re–C(2)	176.2(1)		C(11)–N(1)–C(15)	117.6(3)	
N(1)–Re–O(1)	73.8(1)		C(21)–C(1)–O(1)	119.3(3)	
Re–N(1)–C(11)	116.4(2)		Re–N(1)–C(15)	126.0(2)	
8					
Re–Br(1)	2.523(3)		Re–Br(2)	2.500(3)	
Re–O(1)	1.992(2)		Re–O(2)	2.020(2)	
Re–P(1)	2.463(6)		Re–P(2)	2.475(6)	
C(12)–O(1)	1.325(3)		C(1)–O(2)	1.283(3)	
O(1)–Re–O(2)	85.5(8)		O(2)–Re–Br(1)	172.4(6)	
O(1)–Re–Br(1)	88.4(5)		O(2)–Re–Br(2)	86.7(5)	
O(1)–Re–Br(2)	176.2(1)		O(2)–Re–P(1)	91.1(6)	
O(1)–Re–P(1)	90.6(6)		O(2)–Re–P(2)	88.9(6)	
O(1)–Re–P(2)	90.3(6)		Br(2)–Re–Br(1)	99.6(1)	
Br(1)–Re–P(1)	93.4(2)		Br(2)–Re–P(1)	86.8(2)	
Br(2)–Re–P(2)	86.6(2)		Br(2)–Re–P(2)	92.35(2)	
P(1)–Re–P(2)	179.2(3)		O(2)–C(1)–C(21)	122.0(3)	

	9	**10**		**9**	**10**
Re–X(1)	2.340(5)	2.543(3)	Re–X(2)	2.395(6)	2.482(2)
Re–O(1)	1.966(1)	1.967(2)	Re–O(2)	2.089(1)	2.088(2)
Re–O(3)	1.689(1)	1.675(2)	Re–P(1)	2.472(5)	2.470(6)
C(1)–O(2)	1.262(2)	1.262(3)	C(11)–O(1)	1.336(2)	1.336(3)
O(1)–Re–O(3)	166.0(6)	166.1(8)	O(3)–Re–O(2)	87.5(6)	87.3(7)
O(1)–Re–O(2)	81.0(5)	80.9(7)	O(3)–Re–X(1)	99.3(5)	98.9(6)
O(1)–Re–X(1)	92.9(4)	87.4(5)	O(3)–Re–X(2)	84.3(4)	98.6(6)
O(1)–Re–X(2)	88.3(4)	93.8(5)	O(3)–Re–P(1)	88.3(5)	89.4(6)
O(1)–Re–P(1)	175.1(2)	84.2(5)	O(2)–Re–P(1)	94.0(4)	93.8(5)
O(2)–Re–X(1)	172.2(4)	85.5(4)	X(1)–Re–X(2)	89.2(2)	89.2(1)
O(2)–Re–X(2)	85.9(4)	172.7(4)	X(2)–Re–P(1)	172.8(2)	90.7(2)
X(1)–Re–P(1)	90.1(2)	171.6(2)	O(2)–C(1)–C(12)	122.0(2)	123.0(2)

Table 3
Natural charges of selected atoms for complexes **1** to **10**.

1		**2**		**3**		**4**		**5**	
label/charge									
Re	0.05	Re	1.21	Re	0.85	Re	0.66	Re	1.10
O_1	−0.80	Br_{11}	−0.38	Cl_1	−0.37	Br_1	−0.31	Cl_2	−0.39
N_1	−0.49	Br_{12}	−0.36	Cl_2	−0.40	Br_2	−0.35	Cl_1	−0.46
N_2	−0.50	O_{11}	−0.71	Cl_3	−0.40	Br_3	−0.36	P_1	1.14
C_{30}	0.60	O_{13}	−0.50	P_1	1.11	P_1	1.11	O_1	−0.69
C_{31}	0.51	N_{11}	−0.48	O_1	−0.58	O_1	−0.57	O_2	−0.50
C_{32}	0.60	N_{12}	−0.48	N_1	−0.49	N_1	−0.49	N_1	−0.47
6		**7**		**8**		**9**		**10**	
label/charge									
Re	0.99	Re	0.00	Re	0.52	Re	1.14	Re	1.03
Br_1	−0.34	C_2	0.53	Br_1	−0.41	Cl_1	−0.39	Br_1	−0.37
Br_2	−0.42	C_3	0.59	Br_2	−0.39	Cl_2	−0.42	Br_2	−0.34
P_1	1.15	C_4	0.62	P_1	1.10	P_1	1.14	P_1	1.15
O_1	−0.68	O_1	−0.54	P_2	1.11	O_1	−0.70	O_1	−0.69
O_2	−0.50	N_1	−0.46	O_1	−0.66	O_2	−0.60	O_2	−0.60
N_1	−0.48	Cl_1	−0.56	O_2	−0.60	O_3	−0.41	O_3	−0.40

2.2.6. *cis-*[ReBr$_2$(bp)(PPh$_3$)$_2$] (**8**)

Hbp (408 mg, 206 μmol) was dissolved in 10 cm^3 of methanol, and added to 0.100 g (103 μmol) of *trans*-[ReOBr$_3$(PPh$_3$)$_2$] in 10 cm^3 of methanol. The resulting solution was heated under reflux for an hour and then cooled to room temperature. It was filtered and left to evaporate slowly at room temperature. After 4 days green crystals, suitable for X-ray diffraction studies, were collected by filtration. Yield = 68%, m.p. 267 °C. *Anal.* Calc. for $C_{49}H_{39}Br_2O_2P_2Re$: C, 55.1; H, 3.7. Found: C, 55.2; H, 3.6%. IR (cm^{-1}): ν(C=O) 1630s; ν(Re–O) 436m. Conductivity (DMF): 83.

Table 4
NLMO/NPA bond orders of selected (rhenium–X) bonds for complexes **1** to **10**.

1		**2**		**3**		**4**		**5**	
X(label)/B.O.									
O_1	0.17	Br_{11}	0.55	Cl_1	0.57	Br_1	0.60	Cl_2	0.53
N_1	0.15	Br_{12}	0.54	Cl_2	0.52	Br_2	0.57	Cl_1	0.34
N_2	0.15	O_{11}	0.67	Cl_3	0.48	Br_3	0.50	P_1	0.52
C_{30}	0.89	O_{13}	1.49	P_1	0.41	P_1	0.41	O_1	0.40
C_{31}	1.15	N_{11}	0.51	O_1	0.37	O_1	0.33	O_2	1.45
C_{32}	0.94	N_{12}	0.23	N_1	0.32	N_1	0.37	N_1	0.22
6		**7**		**8**		**9**		**10**	
X(label)/B.O.									
Br_1	0.57	C_2	1.03	Br_1	0.50	Cl_1	0.53	Br_1	0.55
Br_2	0.34	C_3	0.98	Br_2	0.53	Cl_2	0.49	Br_2	0.57
P_1	0.54	C_4	0.92	P_1	0.40	P_1	0.45	P_1	0.36
O_1	0.42	O_1	0.14	P_2	0.39	O_1	0.29	O_1	0.31
O_2	1.46	N_1	0.16	O_1	0.35	O_2	0.20	O_2	0.19
N_1	0.21	Cl_1	0.23	O_2	0.23	O_3	1.60	O_3	1.57

Table 5
Hybrid bond orbitals and lone pairs for complex **1**.

Label	Bond orbital	Occupancy
2c1	$0.5619(sd[2.13])_{Re} + 0.8272(sp[0.56])_{C30}$	1.96
2c2	$0.5767(sd[2.68])_{Re} + 0.8169(sp[0.74])_{C31}$	1.93
2c3	$0.8988(d)_{Re} + 0.4384(p)_{C31}$	1.78
2c4	$0.8874(sd[12.04])_{Re} + 0.4610(sp[12.98])_{C31}$	1.67
2c5	$0.5644(sd[2.16])_{Re} + 0.8255(sp[0.56])_{C32}$	1.96
2c6	$0.9627(d)_{Re} + 0.2706(pd[0.76])_{C32}$	1.63
2c1*	$0.8272(sd[2.13])_{Re} - 0.5619(sp[0.56])_{C30}$	0.28
2c2*	$0.8169(sd[2.68])_{Re} - 0.5767(sp[0.74])_{C31}$	0.30
2c3*	$0.4384(d)_{Re} - 0.8988(p)_{C31}$	0.44
2c4*	$0.4610(sd[12.04])_{Re} - 0.8874(sp[12.98])_{C31}$	0.46
2c5*	$0.8255(sd[2.16])_{Re} - 0.5644(sp[0.56])_{C32}$	0.29
2c6*	$0.2706(d)_{Re} - 0.9627(pd[0.76])_{C32}$	0.21
Label	Lone pair	Occupancy
O_1	sp[0.91], p, sp[5.41]	1.93, 1.87,1.68
N_1	sp[3.24]	1.72
N_2	sp[3.21]	1.72

2.2.7. *cis-*[ReOX$_2$(bp)(PPh$_3$)] (X = Cl(**9**), Br(**10**))

Hbp (240 μmol) was added to a solution of *trans*-[ReOX$_3$(PPh$_3$)$_2$] (120 μmol) in 20 cm^3 of acetonitrile and the mixture was stirred at reflux for 3 h. The color of the reaction mixture turned green and, after cooling to room temperature, the solution was filtered and left to evaporate slowly at room temperature. After two days green X-ray quality crystals were collected by filtration.

*(**9**):* Yield = 70%, 270 °C. *Anal.* Calc. for $C_{31}H_{24}Cl_2O_3PRe$: C, 50.8; H, 3.3. Found: C, 50.6; H, 3.5%. IR (cm^{-1}): ν(Re=O) 948s; ν(Re–O) 478s; ν(Re–Cl) 306m. ^{1}H NMR (DMSO-d_6, ppm): 7.69 (d, 2H, *H22, H26*); 7.64–7.51 (m, 18H, *H13*, *H23*, *H25*, *PPh$_3$*); 7.01–6.92 (m, 4H, *H14*, *H24*, *H15*, *H16*, *H24*). Conductivity (DMF): 70.

*(**10**):* Yield = 72%, m.p. 275 °C. *Anal.* Calc. for $C_{31}H_{24}Br_2O_3PRe$: C, 45.3; H, 2.9. Found: C, 45.2; H, 3.6%. IR (cm^{-1}): ν(Re=O) 947s; ν(Re–O) 498m. ^{1}H NMR (DMSO-d_6, ppm): 7.75–6.80 (m, 24H). Conductivity (DMF): 75.

2.3. X-ray crystallography

X-ray diffraction studies for all the complexes were performed at 200(2) K using a Bruker Kappa Apex II diffractometer with graphite-monochromated Mo Kα (λ = 0.71073 Å) radiation. Further details are given in Table 1. The structures were solved by direct methods. Non-hydrogen atoms were refined with anisotropic displacement parameters; hydrogen atoms bound to carbon were idealized and fixed. Complex **1** was refined with an extinction parameter. Complexes **2**, **3**, **5**, **6**, **8**, **9** and **10** had one or more reflections omitted that were partially obscured by the beam stop. Complex **7** has solvent toluene disordered at a special position. The toluene ring was constrained to a regular hexagon with AFIX 66. Complex **8** has been refined as an inversion twin. Numerical

Table 6
Hybrid bond orbitals and lone pairs for complex **2**.

Label	Bond orbital	Occupancy
2c1	$0.5140(\mathrm{sd}[1.49])_{\mathrm{Re}} + 0.8578(\mathrm{sp}[6.33])_{\mathrm{Br11}}$	1.94
2c2	$0.4621(\mathrm{sp}[1.07]\mathrm{d}[3.93])_{\mathrm{Re}} + 0.8868(\mathrm{sp}[6.41])_{\mathrm{Br12}}$	1.84
2c3	$0.4163(\mathrm{sp}[2.33]\mathrm{d}[13.02])_{\mathrm{Re}} + 0.9092(\mathrm{sp}[2.68])_{\mathrm{O13}}$	1.89
2c4	$0.5526(\mathrm{d})_{\mathrm{Re}} + 0.8335(\mathrm{p})_{\mathrm{O13}}$	1.97
2c5	$0.5354(\mathrm{d})_{\mathrm{Re}} + 0.8446(\mathrm{p})_{\mathrm{O13}}$	1.93
3C1	$0.2864(\mathrm{sp}[0.63]\mathrm{d}[1.30])_{\mathrm{Re}} + 0.6969(\mathrm{sp}[4.30])_{\mathrm{O11}} + 0.6575(\mathrm{sp}[2.79])_{\mathrm{N11}}$	1.84
2c2*	$0.8868(\mathrm{sp}[1.07]\mathrm{d}[3.93])_{\mathrm{Re}} - 0.4621(\mathrm{sp}[6.41])_{\mathrm{Br12}}$	0.29
2c3*	$0.9092(\mathrm{sp}[2.33]\mathrm{d}[13.02])_{\mathrm{Re}} - 0.4163(\mathrm{sp}[2.68])_{\mathrm{O13}}$	0.30
2c4*	$0.8335(\mathrm{d})_{\mathrm{Re}} - 0.5526(\mathrm{p})_{\mathrm{O13}}$	0.29
2c5*	$0.8446(\mathrm{d})_{\mathrm{Re}} - 0.5354(\mathrm{p})_{\mathrm{O13}}$	0.22
3C1a*	$0.0181(\mathrm{sp}[0.63]\mathrm{d}[1.30])_{\mathrm{Re}} - 0.6901(\mathrm{sp}[4.30])_{\mathrm{O11}} - 0.7235\ (\mathrm{sp}[2.79])_{\mathrm{N11}}$	1.62
3C1b*	$0.9579(\mathrm{sp}[0.63]\mathrm{d}[1.30])_{\mathrm{Re}} - 0.1953(\mathrm{sp}[4.30])_{\mathrm{O11}} + 0.2102(\mathrm{sp}[2.79])_{\mathrm{N11}}$	0.23
Label	Lone pair	Occupancy
Re	d	1.92
Br_{11}	sp[0.16], p, p	1.99, 1.98, 1.88
Br_{12}	sp[0.17], p, p	1.99, 1.98, 1.87
O_{13}	sp[0.47]	1.96

absorption corrections were made with SADABS [9]. Structural refinements were carried out by the full-matrix least-squares method on F^2 using the program SHELXL-97 [10].

2.4. Theoretical approach and computational details

DFT was used as implemented in the Firefly quantum chemistry package [11] to calculate the relaxed structures, natural bond orbital (NBO) charges, atom–atom net linear natural localized molecular orbital/natural population analysis (NLMO/NPA) bond orders and hybrid natural bond orbitals of the rhenium complexes [12]. The pre-compiled NBO 5.0 code [12] was employed in Firefly to do the post-processing analyses. The B3LYP hybrid DFT method [13,14], which includes 20% exact exchange and involves three semi-empirical parameters that were obtained by fits to experimental thermochemical data was employed in this work. The 6-31+g(d,p) and 6-31g(d,p) basis sets and LANL2DZ relativistic core potential and double zeta basis set were used for "H, Cl, O, P, N", "C", and "Re, Br" sets respectively [15]. Yeguas et al. have used the same level of theory and basis sets to investigate some rhenium complexes [16]. DFT calculations and NBO analysis has been employed widely to investigate the systems containing metallic and non-metallic elements [17–21]. Tangoulis and co-workers showed that the NLMO/NPA method used in this work gives bond orders which are in better agreement with the chemical nature of the bonds involving transition metals [22]. Calculated natural charges, NLMO/NPA bond orders, hybrid bond orbitals and lone pairs for complexes **1** to **10** are given in 3–11 respectively.

3. Results and discussion

3.1. *fac*-[Re(CO)$_3$(dpk·OCH$_3$)] (**1**)

The compound was prepared by the reaction of [Re(CO)$_5$Cl] with two equivalents of di-2-pyridyl ketone (dpk) in refluxing methanol under nitrogen. The equation for the reaction is

$$[\mathrm{Re(CO)_5Cl}] + \mathrm{dpk} + \mathrm{MeOH} \rightarrow fac\text{-}[\mathrm{Re(CO)_3(dpk \cdot OCH3)}] + \mathrm{HCl} + 2\mathrm{CO}$$

The nucleophilic attack of the solvent at the carbonylic carbon atom to give dpk·OCH$_3$ is not surprising; it was previously shown in the coordination chemistry of dpk with copper complexes [23a]. *fac*-[Re(CO)$_3$(dpk)Cl] was isolated from the reaction of [Re(CO)$_5$Cl] with dpk in refluxing toluene [23b], and the *fac*-[Re(CO)$_3$(dpk·OH)] derivative was formed when [Re(CO)$_3$(dpk)Cl] was suspended in ethanol in the presence of water [6].

Complex **1** is stable in air and in solution for months and is a non-electrolyte in methanol. It is soluble in a wide range of solvents including DMF, DMSO, dichloromethane and alcohols. The infrared spectrum is characterized by intense bands at 2007, 1914 and 1857 cm^{-1}, typical of ν(C=O) of the *fac*-[Re(CO)$_3$]$^+$ unit [24]. The absence of the strong ketonic ν(C=O) stretching frequency in the 1630–1780 cm^{-1} region further supports the metal-promoted nucleophilic attack of methanol on the ketonic group. The coordination of the pyridyl nitrogens is shown by the shift of ν(C=N) from about 1606 cm^{-1} in the free ligand to 1585 cm^{-1} in the complex. The two medium intensity bands at 484 and 430 cm^{-1} are assigned to ν(Re–N). The ^{1}H NMR spectrum shows sharp, well-resolved peaks. The corresponding proton signals of each pyridine ring of the dpk ligand in the complex are identical, giving the expected doublet-triplet-doublet-triplet set of signals, and implying that the corresponding protons of the two rings of the dpk chelate are magnetically equivalent. The two-proton signal the furthest downfield at 9.23 ppm is ascribed to the magnetically equivalent protons *H15* and *H25*, which reside on the carbon atoms adjacent to the coordinating nitrogen atoms. The UV–Vis spectrum in dichloromethane shows a ligand-to-metal charge transfer band at 377 nm, and an intraligand ($\pi \rightarrow \pi^*$) transition of dpk·OCH$_3$ at 318 nm.

An ORTEP perspective view of the asymmetric unit of **1** is shown in Fig. 1, with selected bond lengths and angles listed in Table 2. The X-ray results show that the rhenium(I) complex contains the chemically robust *fac*-[Re(CO)$_3$]$^+$ core in a distorted octahedral geometry. The metal is coordinated to three carbonyl donors in a *facial* orientation, to the two pyridyl nitrogens N(1) and N(2) and the deprotonated oxygen O(1) of dpk. The Re–CO bond distances [average of 1.913(3) Å] fall in the range observed [1.900(2)–1.928(2) Å] for similar complexes [25,26]. The Re–N(2) bond distance [2.184(3) Å] is slightly longer than the Re–N(1) bond [2.178(3) Å], and these values are close to those in other Re(I)–N(imine) bonds, which typically fall in the range 2.15–2.17 Å [1b,27–29]. The distortion from octahedral ideality in the complex is mainly the result of the *trans* angles, which fall in the range 169.5(1)–172.3(1)° (Table 2). These distortions are mainly the result of the constraints imposed by the tridentate coordination of dpk, which has three bite angles [N(1)–Re–O(1) = 74.8(8)°, N(2)–Re–O(1) = 74.6(8)° and N(1)–Re–N(2) = 82.0(9)°]. The angles

Table 7
Hybrid bond orbitals and lone pairs for complexes **3** and **4**.

3		
Label	Bond orbital (α)	Occupancy
2c1α	0.4915(sd[2.2])$_{\mathrm{Re}}$ + 0.8709(sp[4.04])$_{\mathrm{Cl1}}$	0.98
2c2α	0.4777(sd[2.39])$_{\mathrm{Re}}$ + 0.8785(sp[4.11])$_{\mathrm{Cl2}}$	0.98
2c3α	0.5564(sd[1.57])$_{\mathrm{Re}}$ + 0.8309(sp[2.81])$_{\mathrm{P1}}$	0.94
2c2*α	0.8785(sd[2.39])$_{\mathrm{Re}}$ − 0.4777(sp[4.11])$_{\mathrm{Cl2}}$	0.15
Label	Lone pair (α)	Occupancy
Re	d, d, d	0.98, 0.97, 0.90
Cl$_1$	sp[0.43], sp[9.05], p	0.99, 0.99, 0.98
Cl$_2$	sp[0.32], p, p	0.99, 0.98, 0.98
Cl$_3$	sp[0.89], sp[2.57], p	0.99, 0.99, 0.98
O$_1$	sp[1.99], sp[2.73]	0.98, 0.85
N$_1$	sp[3.07]	0.82
P$_1$	sp[5.61]	0.72
Label	Bond orbital (β)	Occupancy
2c1β	0.4811(sd[4.05])$_{\mathrm{Re}}$ + 0.8767(sp[3.74])$_{\mathrm{Cl1}}$	0.98
2c2β	0.5170(sd[3.61])$_{\mathrm{Re}}$ + 0.8560(sp[4.34]])$_{\mathrm{Cl3}}$	0.98
2c3β	0.4103([d])$_{\mathrm{Re}}$ + 0.9120([p])$_{\mathrm{O1}}$	0.90
2c4β	0.4562([d])$_{\mathrm{Re}}$ + 0.8899([p])$_{\mathrm{N1}}$	0.81
2c1*β	0.8767(sd[4.05])$_{\mathrm{Re}}$ − 0.4811(sp[3.74])$_{\mathrm{Cl1}}$	0.16
2c2*β	0.8560(sd[3.61])$_{\mathrm{Re}}$ − 0.5170(sp[4.34])$_{\mathrm{Cl3}}$	0.25
2c3*β	0.9120([d])$_{\mathrm{Re}}$ − 0.4103([p])$_{\mathrm{O1}}$	0.26
2c4*β	0.8899([d])$_{\mathrm{Re}}$ − 0.4562([p])$_{\mathrm{N1}}$	0.27
Label	Lone pair (β)	Occupancy
Cl$_1$	sp[0.29], p, p	0.99, 0.90, 0.89
Cl$_2$	sp[0.29], p, p, sp[3.84]	0.99, 0.92, 0.90, 0.80
Cl$_3$	sp[0.89], sp[2.57], p	0.99, 0.94, 0.90
P$_1$	sp[5.61]	0.72
O$_1$	sp[1.45], sp[4.13]	0.95, 0.85
N$_1$	sp[3]	0.83
Re*	sd[3.38], sd[1.93]	0.27, 0.22
4		
Label	Bond orbital (α)	Occupancy
2c1α	0.5169(sd[2.21])$_{\mathrm{Re}}$ + 0.8560(sp[5.57])$_{\mathrm{Br1}}$	0.98
2c2α	0.5018(sd[2.35])$_{\mathrm{Re}}$ + 0.8650(sp[5.63])$_{\mathrm{Br2}}$	0.98
2c3α	0.5745(sd[1.60])$_{\mathrm{Re}}$ + 0.8185 sp[2.81])$_{\mathrm{P1}}$	0.95
2c1*α	0.8650(sd[2.35])$_{\mathrm{Re}}$ − 0.5018(sp[5.63])$_{\mathrm{Br2}}$	0.15
Label	Lone pair (α)	Occupancy
Re	d, d, d	0.97, 0.90, 0.98
Br$_1$	sp[0.47], sp[5.11], p	0.98, 0.99, 0.99
Br$_2$	sp[0.24], p, p	0.98, 0.98, 0.99
Br$_3$	sp[6.16], sp[0.44], p	0.99, 0.98, 0.99
N$_1$	sp[3.04]	0.82
Label	Bond orbital (β)	Occupancy
2c1β	0.4979(sd[2.77])$_{\mathrm{Re}}$ + 0.8672(sp[5.09])$_{\mathrm{Br1}}$	0.98
2c2β	0.4827(sd[2.97])$_{\mathrm{Re}}$ + 0.8758(sp[5.14])$_{\mathrm{Br2}}$	0.98
2c3β	0.5244(sd[1.81])$_{\mathrm{Re}}$ + 0.8515(sp[5.92])$_{\mathrm{Br3}}$	0.98
2c4β	0.6035(d)$_{\mathrm{Re}}$ + 0.7974(p)$_{\mathrm{N1}}$	0.87
2c1β*	0.7974(d)$_{\mathrm{Re}}$ − 0.6035(p)$_{\mathrm{N1}}$	0.38
2c2β*	0.8672(sd[2.77])$_{\mathrm{Re}}$ − 0.4979(sp[5.09])$_{\mathrm{Br1}}$	0.15
2c3β*	0.8758(sd[2.97])$_{\mathrm{Re}}$ − 0.4827(sp[5.14])$_{\mathrm{Br2}}$	0.13
2c4β*	0.8515(sd[1.81])$_{\mathrm{Re}}$ − 0.5244(sp[5.92])$_{\mathrm{Br3}}$	0.24
Label	Lone pair (β)	Occupancy
Br$_1$	sp[0.22], p, p	0.89, 0.89, 0.99
Br$_2$	sp[0.22], p, p	0.90, 0.92, 0.99
Br$_3$	sp[0.18], p, p	0.95, 0.90, 0.99
N$_1$	sp[2.98]	0.83
Re*	d, sd[7.38]	0.25, 0.23

Table 8
Hybrid bond orbitals and lone pairs for complexes **5** and **6**.

5		
Label	Bond orbital	Occupancy
2c1	0.5191(sd[4.23])$_{\mathrm{Re}}$ + 0.8547(sp[4.49])$_{\mathrm{Cl2}}$	1.97
2c2	0.5795(sd[3.34])$_{\mathrm{Re}}$ + 0.8150(sp[2.84])$_{\mathrm{P1}}$	1.91
2c3	0.5581(d)$_{\mathrm{Re}}$ + 0.8298(sp[9.63])$_{\mathrm{O2}}$	1.98
2c4	0.5650(d)$_{\mathrm{Re}}$ + 0.8251(p)$_{\mathrm{O2}}$	1.98
2c1*	0.8547(sd[4.23])$_{\mathrm{Re}}$ − 0.5191(sp[4.49])$_{\mathrm{Cl2}}$	0.39
2c2*	0.8150(sd[3.34])$_{\mathrm{Re}}$ − 0.5795(sp[2.84])$_{\mathrm{P1}}$	0.52
2c3*	0.8298(d)$_{\mathrm{Re}}$ − 0.5581(sp[9.63])$_{\mathrm{O2}}$	0.27
2c4*	0.8251(d)$_{\mathrm{Re}}$ − 0.5650(p)$_{\mathrm{O2}}$	0.30
Label	Lone pair	Occupancy
Re	d	1.91
Cl$_2$	sp[0.22], p, p	1.99, 1.98, 1.86
Cl$_1$	sp[0.34], sp[8.86], p, sp[5.53]	1.99, 1.98, 1.90, 1.56
O$_2$	sp[0.50], sp[2.73]	1.96, 1.62
O$_1$	sp[1.02], p, sp[4.61]	1.89, 1.76, 1.68
N$_1$	sp[3.07], p	1.66, 1.30
Re*	sd[0.79]	0.48
6		
Label	Bond orbital	Occupancy
2c1	0.5451(sd[3.72])$_{\mathrm{Re}}$ + 0.8384(sp[6.30])$_{\mathrm{Br1}}$	1.97
2c2	0.5966(sd[3.25])$_{\mathrm{Re}}$ + 0.8026(sp[2.89])$_{\mathrm{P1}}$	1.92
2c3	0.5598(sd[98.19])$_{\mathrm{Re}}$ + 0.8286(sp[10.65])$_{\mathrm{O2}}$	1.98
2c4	0.5649(d)$_{\mathrm{Re}}$ + 0.8252(p)$_{\mathrm{O2}}$	1.98
2c1*	0.8384(sd[3.72])$_{\mathrm{Re}}$ − 0.5451(sp[6.30])$_{\mathrm{Br1}}$	0.39
2c2*	0.8026(sd[3.25])$_{\mathrm{Re}}$ − 0.5966(sp[2.89])$_{\mathrm{P1}}$	0.56
2c3*	0.8286(d)$_{\mathrm{Re}}$ − 0.5598(sp[10.65])$_{\mathrm{O2}}$	0.26
2c4*	0.8252(d)$_{\mathrm{Re}}$ − 0.5649(p)$_{\mathrm{O2}}$	0.30
Label	Lone pair	Occupancy
Re	d	1.92
Br$_1$	sp[0.16], p, p	1.99, 1.97, 1.87
Br$_2$	sp[0.36], sp[5.65], p, sp[7.86]	1.99, 1.98, 1.92, 1.52
O$_2$	sp[0.51], sp[2.99]	1.96, 1.63
O$_1$	sp[1.01], p[1.76], sp[4.80]	1.89, 1.76, 1.69
N$_1$	sp[3.23]	1.66
Re*	sd[0.88]	0.49

Table 9
Hybrid bond orbitals and lone pairs for complex **7**.

Label	Bond orbital	Occupancy
2c1	0.5676(sd[2.38])$_{\mathrm{Re}}$ + 0.8233(sp[0.6])$_{\mathrm{C2}}$	1.96
2c2	0.9056(d)$_{\mathrm{Re}}$ + 0.4240(p)$_{\mathrm{C2}}$	1.80
2c3	0.9060(d)$_{\mathrm{Re}}$ + 0.4232(p)$_{\mathrm{C2}}$	1.71
2c4	0.5759(sd[2.83])$_{\mathrm{Re}}$ + 0.8175(sp[0.56])$_{\mathrm{C3}}$	1.97
2c5	0.5757(sd[2.60])$_{\mathrm{Re}}$ + 0.8177(sp[0.56])$_{\mathrm{C4}}$	1.97
2c1*	0.8233(sd[2.38])$_{\mathrm{Re}}$ − 0.5676(sp[0.6])$_{\mathrm{C2}}$	0.37
2c2*	0.4240(d)$_{\mathrm{Re}}$ − 0.9056(p)$_{\mathrm{C2}}$	0.44
2c3*	0.4232(d)$_{\mathrm{Re}}$ − 0.9060(p)$_{\mathrm{C2}}$	0.45
2c4*	0.8175(sd[2.83])$_{\mathrm{Re}}$ − 0.5759(sp[0.56])$_{\mathrm{C3}}$	0.31
2c5*	0.8177(sd[2.60])$_{\mathrm{Re}}$ − 0.5757(sp[0.56])$_{\mathrm{C4}}$	0.35
Label	Lone pair	Occupancy
Re	sd[6.24]	1.35
O$_1$	sp[1.69], sp[3.74]	1.95, 1.78
N$_1$	sp[3.07]	1.73
Cl$_1$	sp[0.28], p, p, sp[4.96]	1.99, 1.97, 1.96, 1.63

around C(1) [O(1)–C(1)–O(2) = 114.4(2)°; O(1)–C(1)–C(11) = 107.4(2)°; O(1)–C(1)–C(21) = 108.5(2)°] are further evidence of the rehybridization of C(1) from *sp*^{2} in free dpk to *sp*^{3} in the complex.

The theoretical calculations show that the ground state of **1** is singlet and that the electronic configuration of rhenium is [core]6s(0.41)5d(6.55). The rhenium uses sd$^{2.1}$ and sd$^{2.7}$ hybrid electrons to bind to the carbon atoms and does not have any lone pair electrons. However, the 2c3, 2c4, and 2c6 hybrid bond orbitals show that the shared electrons are mainly localized on the rhenium. The Re–O(1) and both Re–N bond orders are small and the second order perturbation theory analysis of the Fock matrix shows that the O and N lone pair electrons are delocalized on Re–C anti bond orbitals. The Re–N(2) and Re–N(1) calculated bond distances are 2.239 and 2.232 Å respectively. They are in good agreement with the experimental results which show the former

Table 10
Hybrid bond orbitals and lone pairs for complex **8**.

Label	Bond orbital (α)	Occupancy
2c1	0.4988(sd[2.59])$_{Re}$ + 0.8667(sd[5.35])$_{Br1}$	0.98
2c2	0.4921(sd[2.55])$_{Re}$ + 0.8705(sp[5.20])$_{Br2}$	0.98
2c3	0.5604(sd[1.29])$_{Re}$ + 0.8282(sp[2.38])$_{P1}$	0.95
2c1*	0.8667(sd[2.59])$_{Re}$ – 0.4968(sp[5.35])$_{Br1}$	0.14
2c2*	0.8705(sd[2.55])$_{Re}$ – 0.4921(sp[5.20])$_{Br2}$	0.16
2c3*	0.8282(sd[1.29])$_{Re}$ – 0.5604(sp[2.38])$_{P1}$	0.26
Label	Lone pair (α)	Occupancy
Re	d, d, d	0.99, 0.97, 0.92
Br$_1$	sp[0.23], p, p	0.99, 0.99, 0.98
Br$_2$	sp[0.51], sp[4.66], p	0.99, 0.99, 0.99
P$_2$	sp[5.17]	0.70
O$_1$	sp[2.68], sp[6.40], sp[3.99]	0.98, 0.89, 0.84
O$_2$	sp[2.94], sp[2.07]	0.97, 0.87
Label	Bond orbital (β)	Occupancy
2c1	0.4731(sd[2.85])$_{Re}$ + 0.8818(sp[4.57])$_{Br1}$	0.98
2c2	0.4611(sd[2.79])$_{Re}$ + 0.8873(sp[4.45])$_{Br2}$	0.97
2c3	0.5399(sd[1.53])$_{Re}$ + 0.8417(sp[2.39])$_{P2}$	0.95
2c4	0.3742(sp[2.18])$_{Re}$ + 0.9274(p)$_{O1}$	0.89
2c1*	0.8810(sd[2.85])$_{Re}$ – 0.4731(sp[4.57])$_{Br1}$	0.25
2c2*	0.8873(sd[2.79])$_{Re}$ – 0.4611(sp[4.45])$_{Br2}$	0.13
2c3*	0.8417(sd[1.53])$_{Re}$ – 0.5399(sp[2.39])$_{P2}$	0.14
2c4*	0.9274(sp[2.18])$_{Re}$ – 0.3742(p)$_{O1}$	0.14
Label	Lone pair (β)	Occupancy
Re	d	0.84
Br$_1$	sp[0.22], p, p	0.99, 0.97, 0.92
Br$_2$	sp[0.23], p, p	0.99, 0.93, 0.90
P$_1$	sp[4.46]	0.72
O$_1$	sp[1.64], sp[3.49]	0.95, 0.85
O$_2$	sp[2.01], sp[3.09]	0.95, 0.86

Table 11
Hybrid bond orbitals and lone pairs for complexes **9** and **10**.

9		
Label	Bond orbital	Occupancy
2c1	0.4907(sd[1.61])$_{Re}$ + 0.8713(sp[4.89])$_{Cl1}$	1.94
2c2	0.3758(sp[1.72]d[1.99])$_{Re}$ + 0.9267(sp[5.61])$_{Cl2}$	1.76
2c3	0.4138(sp[1.91]d[1.96])$_{Re}$ + 0.9104(sp[2.91])$_{P1}$	1.68
2c4	0.4766(sd[3.47])$_{Re}$ + 0.8791(sp[2.79])$_{O3}$	1.96
2c5	0.5596(d)$_{Re}$ + 0.8287(p)$_{O3}$	1.98
2c6	0.5595(d)$_{Re}$ + 0.8288(p)$_{O3}$	1.94
2c1*	0.8713(sd[1.61])$_{Re}$ – 0.4907(sp[4.89])$_{Cl1}$	0.26
2c2*	0.9267(sp[1.72]d[1.99])$_{Re}$ – 0.3758(sp[5.61])$_{Cl2}$	0.28
2c3*	0.9109(sp[1.91]d[1.96])$_{Re}$ – 0.4138(sp[2.91])$_{P1}$	0.28
2c4*	0.8791(sd[3.47])$_{Re}$ – 0.4766(sp[2.79])$_{O3}$	0.28
2c5*	0.8287(d)$_{Re}$ – 0.5596(p)$_{O3}$	0.26
2c6*	0.8288(d)$_{Re}$ – 0.5259(p)$_{O3}$	0.25
Label	Lone pair	Occupancy
Re	d	1.91
Cl$_1$	sp[0.22], p, p	1.99, 1.98, 1.87
Cl$_2$	sp[0.21], p, p	1.99, 1.98, 1.88
O$_1$	sp[1.64], sp[4.13], p	1.89, 1.76, 1.61
O$_2$	sp[1.99], sp[3.17]	1.93, 1.74
O$_3$	sp[0.48]	1.97
10		
Label	Bond orbital	Occupancy
2c1	0.5489(sd[1.32])$_{Re}$ + 0.8359(sp[8.08])$_{Br1}$	1.94
2c2	0.5236(sd[1.79])$_{Re}$ + 0.8519(sp[7.00])$_{Br2}$	1.94
2c3	0.4799(sd[4.29])$_{Re}$ + 0.8773(sp[2.85])$_{O3}$	1.96
2c4	0.5665(d)$_{Re}$ + 0.8241(p)$_{O3}$	1.99
2c5	0.5815(d)$_{Re}$ + 0.8135(p)$_{O3}$	1.99
2c1*	0.8359(sd[1.32])$_{Re}$ – 0.5489(sp[8.08])$_{Br1}$	0.49
2c2*	0.8519(sd[1.79])$_{Re}$ – 0.5236(sp[7.00])$_{Br2}$	0.27
2c3*	0.8773(sd[4.29])$_{Re}$ – 0.4799(sp[2.85])$_{O3}$	0.29
2c4*	0.8241(d)$_{Re}$ – 0.5665(p)$_{O3}$	0.26
2c5*	0.8135(d)$_{Re}$ – 0.5815(p)$_{O3}$	0.28
Label	Lone pair	Occupancy
Re	d	1.92
Br$_1$	sp[0.19], p, p	1.99, 1.98, 1.89
Br$_2$	sp[0.15], p, p	1.99, 1.98, 1.88
P$_1$	sp[6.55]	1.36
O$_1$	sp[1.61], sp[4.25], p	1.89, 1.76, 1.69
O$_2$	sp[1.92], sp[3.26]	1.93, 1.74
O$_3$	sp[0.48]	1.97

bond length to be slightly larger. As shown in Table 4, the Re–O(1) bond order is small, which confirms the considerably large bond distance seen experimentally. The natural charge of rhenium is +0.05, which is consistent with the presence of less electronegative ligands in this complex, compared to complexes **2** and **3**.

3.2. *cis*-[ReOBr$_2$(dpk·OH)]·2(dpkH$^+$Br$^-$) (**2**)

The complex adduct was isolated from the heating under reflux of *trans*-[ReOBr$_3$(PPh$_3$)$_2$] with a twofold molar excess of dpk in acetone in air. The same adduct was reported previously (erroneously as [ReOBr$_3$(dpk·OH)]·2{dpkH$^+$Br$^-$}), with recrystallization from acetonitrile [5a]. Upon complex formation, dpk undergoes nucleophilic attack by water at the carbonylic carbon atom to form a *gem*-diol form of dpk·OH, which is coordinated to the rhenium(V) as a N,N,O-donor chelate.

The complex is stable in air and is soluble in a wide range of solvents including DMF, DMSO, acetone and acetonitrile. A very intense band in the solid state infrared spectrum at 950 cm^{-1} is attributable to the Re=O stretching frequency, which is close to the observed region of 906–948 cm^{-1} for neutral six-coordinate oxorhenium(V) compounds with an alcoholate oxygen atom coordinated *trans* to the oxo group [30]. The absorption bands at 1693 cm^{-1} is due to ν(C=O) of the protonated dpk molecules in the outer coordination sphere. The typical pyridinic C=N and C=C stretching vibrations give rise to strong absorptions at 1605 and 1520 cm^{-1} respectively. There is a very broad absorption band at 3086 cm^{-1}, which can be assigned to the ν(OH) stretching frequency, confirming the monoanionic *gem*-diol form of dpk·OH in the coordination sphere. The two absorption bands at 470 and 465 cm^{-1} are attributable to ν(Re–N) of the pyridine nitrogens. In the ^{1}H NMR of the complex the lack of paramagnetic broadening confirms the diamagnetic character of **2**. The spectrum is complicated due to the presence of the two uncoordinated molecules of dpkH$^+$ in the compound. However, the aromatic region integrates for 24 protons. The doublet the furthest downfield at 8.70 ppm integrates for two protons, and is ascribed to the magnetically equivalent protons *H115* and *H125* of the coordinated dpk·OH ligand. The four-proton doublet centered at 8.38 ppm is assigned to the protons on the carbons adjacent to the nitrogens of the two free dpkH$^+$ molecules. There are triplets at 7.68 ppm (one proton each on *C113* and *C124*) and at 7.78 ppm (four protons on uncoordinated dpkH$^+$ molecules), and a twelve-proton multiplet in the range 7.95–8.13 ppm.

The asymmetric unit of **2** comprises of the oxorhenium(V) complex *cis*-[ReOBr$_2$(dpk·OH)] (Fig. 2), two bromide anions and two dpkH$^+$ molecules. The donor atoms surrounding the rhenium are at the apices of a distorted octahedron, in which the equatorial plane is occupied by the two *cis* bromine atoms Br(11) and Br(12) and the two terminal pyridyl nitrogen atoms of the tridentate ligand N(11) and N(12), with the O(13) oxo ligand coordinated *trans* to the deprotonated oxygen O(11) of dpk·OH, which acts as a uninegative, tridentate N,O,N-donor ligand. Severe distortions from an ideal rhenium-centered octahedral environment results in a non-linear N(12)–Re–Br(11) axis of 168.0(5)°, with the other *trans* angles Br(12)-Re–N(11) = 166.6(5)° and O(11)–Re–O(13) = 157.0(7)° also deviating from linearity (Table 2). The rhenium atom lies 0.169 Å out of the mean equatorial plane towards O(13), with

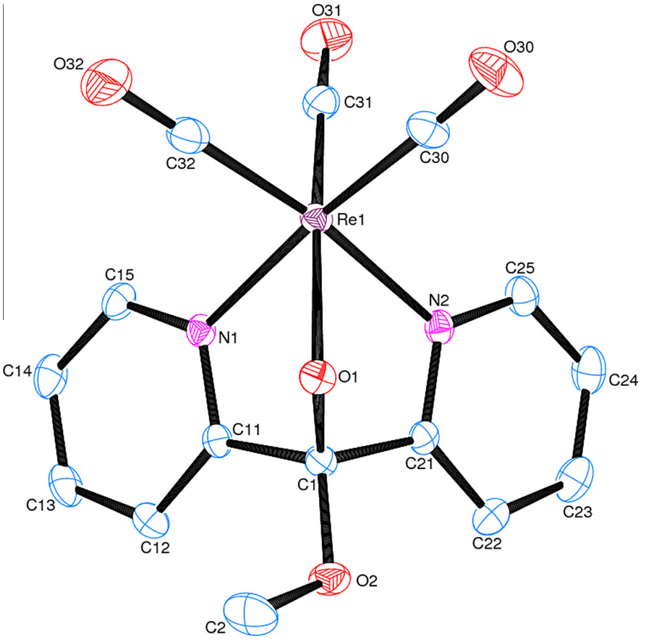

Fig. 1. ORTEP plot of *fac*-[Re(CO)$_3$(dpk·OCH$_3$)] (**1**) showing the atom labeling; thermal ellipsoids are drawn at 50% probability.

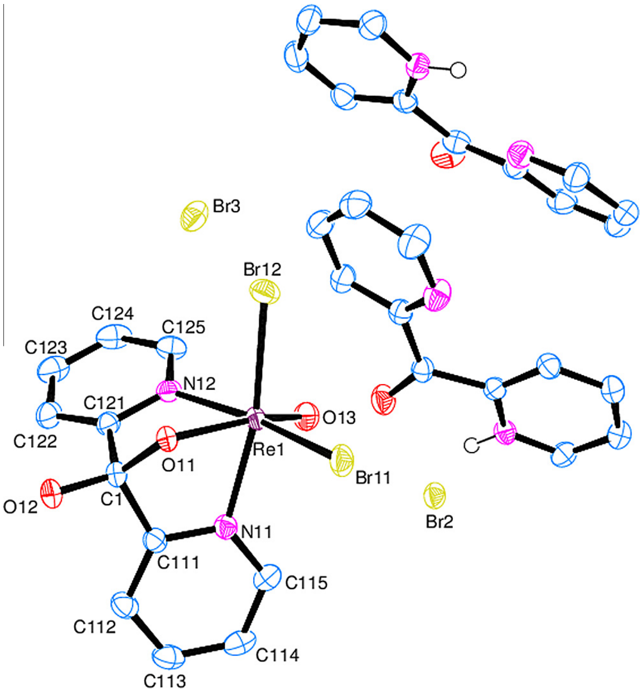

Fig. 2. ORTEP plot of *cis*-[ReOBr$_2$(dpk·OH)] showing the atom labeling; thermal ellipsoids are drawn at 50% probability. Hydrogen atoms are omitted for clarity.

the angles O(13)–Re–Br(11) = 103.7(6)°, O(13)–Re–Br(12) = 102.6(6)°, O(13)–Re–N(11) = 90.0(8)° and O(13)–Re–N(12) = 87.8(8)°. The three bite angles of the chelate are O(11)–Re–N(11) = 74.2(7)°, O(11)–Re–N(12) = 74.4(7)° and N(11)–Re–N(12) = 84.9(7)°. As expected, the bite angle formed by the six-membered metallocycle [N(11)–Re–N(12)] is larger than those of the five-membered ones.

Bond lengths and angles show no unusual features, being within the range expected from the comparison of other six-coordinate mono-oxo complexes of rhenium(V). The Re=O(13) bond length of 1.682(2) Å is within the range observed for oxorhenium(V) compounds [1,31]. The Re–O(11) bond length of 1.966(1) Å is substantially shorter than the usual length for a Re–O single bond [2.04 Å] which illustrates the delocalization of the π-electron density from the oxo bond to the *trans* Re–O bond [32,33]. The average Re–N bond length of 2.147(2) Å is typical of the rhenium(V)-pyridyl bonds [34,35], and they are slightly shorter than those in complex **1**. On average, the two pyridyl rings make a dihedral angle of 83.26° with the mean equatorial planes, and 64.69° with each other. The N–C–C angles at the ring junctions deviate significantly from 120° [N(11)–C(111)–C(1) = 110.7(2)°; N(12)–C(121)–C(1) = 110.8(2)°], and the rhenium atom lies off the lone-pair directions of 120° [C(111)–N(11)–Re(1) = 112.7(2)°; C(121)–N(12)–Re(1) = 113.2(1)°]. There is a remarkable difference between the O(11)–C(1) bond length [1.403(2) Å] and the O(12)–C(1) length of 1.368(3) Å, with C(1) being sp^3 hybridized [O(11)–C(1)–C(111) = 105.4(2)°] and [O(12)–C(1)–C(111) = 110.3(2)°].

The theoretical calculations show that the ground state of **2** is a singlet and that the rhenium's electronic configuration is [core]6s(0.38)5d(5.35). From data in Table 6 it is clear that the bromine (2c1, 2c2) and oxygen donor atoms (2c3, 2c4) use p electrons for their bond formation to rhenium. The three 2c3, 2c4, and 2c5 bond orbitals and the large Re–O(13) bond order are in accordance with the experimental IR data. N(11) shares $sp^{2.79}$ electrons with O(11) and the rhenium electrons to make a three-center bond orbital, but the N(12) lone pair electrons are delocalized on the Re-Br(11) anti bond orbital. The Re–N(11) and Re–N(12) calculated bond distances are 2.185 and 2.179 Å respectively. All ligands in the complex are electronegative which results in a large natural charge of +1.21 on the rhenium.

3.3. [ReX$_3$(zpy)(PPh$_3$)] (**3** and **4**)

The reactions of *trans*-[ReOX$_3$(PPh$_3$)$_2$] (X = Cl, Br) with a twofold molar excess of 2-benzoylpyridine (zpy) in acetonitrile, heated at reflux in air, gave rhenium(III) complexes of the type [ReX$_3$(zpy)(PPh$_3$)] [X = Cl (**3**); Br (**4**)], which were formed by the reduction of rhenium(V) to (III) according to the equation

$$[\mathrm{Re^{V}OX_3(PPh_3)_2}] + \mathrm{zpy} \rightarrow [\mathrm{Re^{III}X_3(zpy)(PPh_3)}] + \mathrm{OPPh_3}$$

It is well known that [ReOX$_3$(PPh$_3$)$_2$] is reduced to [ReX$_3$(MeCN)(PPh$_3$)$_2$] in acetonitrile by PPh$_3$ in the absence of ligands. The latter complex has been shown to be a useful precursor for the preparation of Re(III) coordination compounds [22]. In fact, complexes **3** and **4** were synthesized previously by the reactions of [ReX$_3$(MeCN)(PPh$_3$)$_2$] with equimolar amounts of zpy in dichloromethane [7a]. In both the synthetic reactions of **3** and **4** the colors of the starting materials changed to dark blue after heating for 90 min, and when heating was stopped after 3 h, blue precipitates were collected in good yields. The elemental analyses of the complexes are in good agreement with their formulations. The complexes are soluble in a variety of solvents including acetone, acetonitrile, dichloromethane and DMF. They are insoluble in alcohols and benzene. They are both stable for months in the solid state and for days in solution.

The absence of the typical $\mathrm{Re^{V}{=}O}$ stretching frequency in the 890–1020 cm^{-1} region implies that rhenium(III) products have formed. The neutral bidentate coordination of zpy through the ketonic oxygen in the coordination sphere of the complexes is supported by the shift of the ν(C=O) at 1667 cm^{-1} in the free ligand to 1590 and 1589 cm^{-1} in **3** and **4** respectively. The Re–N stretches appear at 499 and 495 cm^{-1}, and the Re–O ones at 427 and 425 cm^{-1}, in **3** and **4** respectively. The ^{1}H NMR spectra of the complexes are identical, with the halides having no influence on the signals. As zpy consists of two different ring systems, the expected splitting of doublet-triplet-doublet-triplet is observed for the pyridine protons. A one-proton doublet the furthest downfield at 8.73 ppm is assigned to the proton on C25 in complex **3** and on C15 in complex **4**. A fifteen-proton multiplet in the range 7.62–7.59 ppm illustrates the presence of the phosphine molecule. The blue color of the complexes leads to intense absorption bands in the visible region of their electronic spectra. Due to their high extinction coefficients, the absorptions at 428 nm (**3**) and 468 nm (**4**) are probably due to $d_\pi Re(III) \rightarrow \pi^*(zpy)$ metal-to-ligand charge transfer transitions. The spectra are dominated by an intense absorption (around 300 nm) due to the $\pi \rightarrow \pi^*$ transition of the aromatic rings in zpy. The d–d transitions are also observed at 597 and 611 nm in **3** and **4** respectively.

Single crystals of X-ray quality were obtained by slow evaporation from the acetonitrile mother liquor. The crystal structures show that the rhenium ion lies at the center of a distorted octahedron (Figs. 3 and 4). The basal planes are defined by the two halides X(1) and X(2), the ketonic oxygen O(1) and the pyridyl nitrogen N(1) of zpy. The phosphorus atom P and X(3) lie in *trans* axial positions. Distortion from an ideal octahedral environment results in a non-linear N(1)–Re–X(1) axis of 167.9(7)° in **3** and 169.4(8)° in **4**, with the other *trans* angles X(2)–Re–O(1) = 172.0(6)° and 171.3(7)° and P(1)–Re–X(3) = 177.3(3)° and 176.1(3)° in **3** and **4** respectively. The bite angle [O(1)-Re–N(1) = 75.5(9)° in **3** and 75.6(1)° in **4**] of zpy is practically identical in both complexes, and it contributes significantly to the distortion in the complexes. The large X(1)–Re–X(2) angle of 95.1(3)° and 94.4(1)° in **3** and **4** respectively may contribute to the smaller bite angle of zpy.

The halide ions are arranged in a *facial* fashion, typical of the $[ReX_3(L\text{-}L)(PPh_3)]$ compounds with bipy-like ligands [36]. The back-bonding effect of the complexes $[ReX_3(L\text{-}L)(PPh_3)]$ with two π-acceptor ligands coordinated to a π-donor rhenium(III) center is maximized in the *facial* disposition, which ensures minimum competition between the ligands for identical metal orbitals. The O(1)=C(2) bond [1.286(3) Å average] is weakened and longer than the C=O [1.213(2) Å] in the free ligand [37], but is within the expected range for similar complexes [38]. The Re–N distance of 2.062(2) Å in **3** is shorter than comparable distances for saturated amine complexes, where metal-to-ligand π-back-bonding is not possible [28]. Similarly, the interatomic distance between the rhenium atom and the oxygen atom of zpy [2.001(2) Å in **3**] is shorter than an ideal single Re–O bond length of 2.04 Å [39]. The latter is also observed in complex **4**. The Re–X(3) bond distances, *trans* to P(1), are significantly longer than the Re–X bond distances *trans* to the nitrogen and oxygen donor atoms of zpy (Table 2). All these data suggest that the zpy chelate acts as a bidentate ligand, with the rhenium in the +III oxidation state.

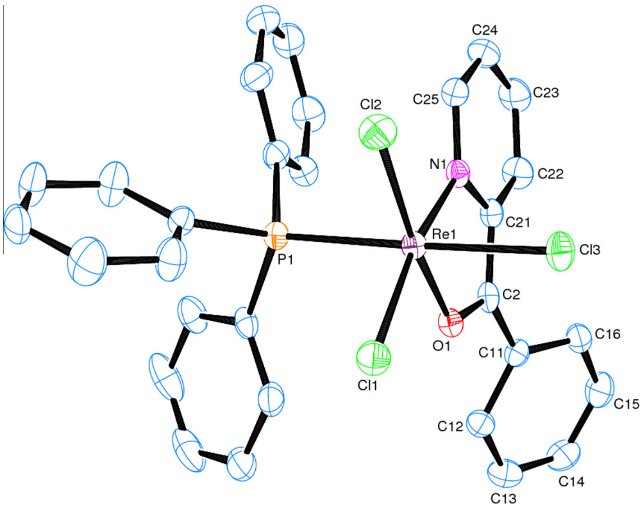

Fig. 3. ORTEP view of **3** showing the atom labeling scheme. Atomic ellipsoids are drawn at the 40% probability level.

It was shown previously that the reaction of 1-isoquinolinyl phenyl ketone (qpk) with $[ReCl_3(MeCN)(PPh_3)_2]$ led to the isolation of the species $[ReCl_3(qpk)(PPh_3)]$, in which the coordination of qpk occurs through the neutral ketonic oxygen atom [Re–O = 1.990 (3) Å] and the quinolinyl nitrogen [Re–N = 2.026(3) Å] [27].

The theoretical calculations show that the ground state of **3** and **4** are triplet and that the electronic configuration of rhenium is [core]6s(0.38)5d(5.70) and [core]6s(0.45)5d(5.82) respectively. The rhenium uses more d and less s electrons to form bonds with the three halides, which mainly share their p electrons rather than their s electrons. According to the data in Table 7 for the bond orbital 2c1α in complex **3** $(sp[4.04])_{Cl1}$ and **4** $(sp[5.57]_{Br1})$, the bromines use a larger percentage of their p electrons than the chlorines in forming bonds to the metal. In these Re–halide bond orbitals the ligands have large polarization coefficients (~0.8). The 2c3β bond orbital and the corresponding anti bond orbital in **3** prove the absence of a strong Re=O double bond. Although we couldn't find any local bond orbital between the rhenium and the oxygen in **4**, the second order perturbation theory analysis of Fock matrix shows delocalization of the C-O bond orbital and the oxygen lone pairs on Re-Br anti bond orbitals. Overall, the Re–O bond order in these cases proves the lack of a strong double bond and is in agreement with our experimental data. The calculated Re–N bond distances of 2.091 and 2.093 Å in **3** and **4** are in good agreement with experiment. The C–O bond orders in **3** and **4** are 0.93 and 1.04 respectively, almost twice the mean Re-ligand bond order. The calculated C–O bond distances in **3** and **4** are 1.292 and 1.289 Å respectively. All donor atoms gain negative natural charges except phosphorus, which is caused by forming more than three bonds (with the carbon atoms and the transition metal). The natural charge of rhenium in **3** is more positive than in **4**, which is consistent with the presence of more electronegative ligands in the former.

3.4. $[ReOX_2(zpyH)(PPh_3)]$ (**5** and **6**)

The reactions of *trans*-$[ReOX_3(PPh_3)_2]$ (X = Cl, Br) with 2-benzoylpyridine (zpy) in methanol in the presence of air produced the neutral oxorhenium(V) complexes of the type $[ReOX_2(zpyH)(PPh_3)]$ [X = Cl(**5**); Br(**6**)]. Both these complexes have been synthesized previously by the reaction of equimolar quantities of $[ReOX_3(PPh_3)_2]$ and zpy in ethanol containing two drops of conc. hydrochloric acid [7b]. During the reaction the 2-benzoylpyridine $[C_6H_5(C{=}O)C_5H_4N]$ molecule was reduced to the phenyl-2-pyridylmethanolate anion [zpyH⁻, $\{C_6H_5(HC\text{-}O)C_5H_4N\}^-$)], which coordinates to the metal center through the deprotonated alcoholate oxygen and the pyridyl nitrogen atom. Examples of the reduction of ketones to alcohols in methanol by rhenium complexes could not be found in the literature. We suggest that the reduction of zpy is of the Meerwein–Ponndorf–Verley type [30], with coordination of both the methoxide and zpy before hydride transfer from the methoxy to the carbonyl carbon of zpy. However, in a similar study the reaction of qpk with $[ReOBr_3(PPh_3)_2]$ in acetone produced the complex $[ReOBr_2(qpk.OH)(PPh_3)]$, in which nucleophilic attack of water has occurred to the carbonylic carbon atom of qpk. The coordination of qpk·OH is in a bidentate monoanionic *gem*-diol form [5b].

The infrared spectra of the complexes display the Re=O stretching frequency at 948 and 944 cm^{-1} in **5** and **6** respectively, which is at the lower end of the range that is normally expected (895–1020 cm^{-1}) for this vibration [40]. The characteristic bands corresponding to the $\nu(C{=}N)$ and $\nu(C{=}C)$ of the ligand are observed

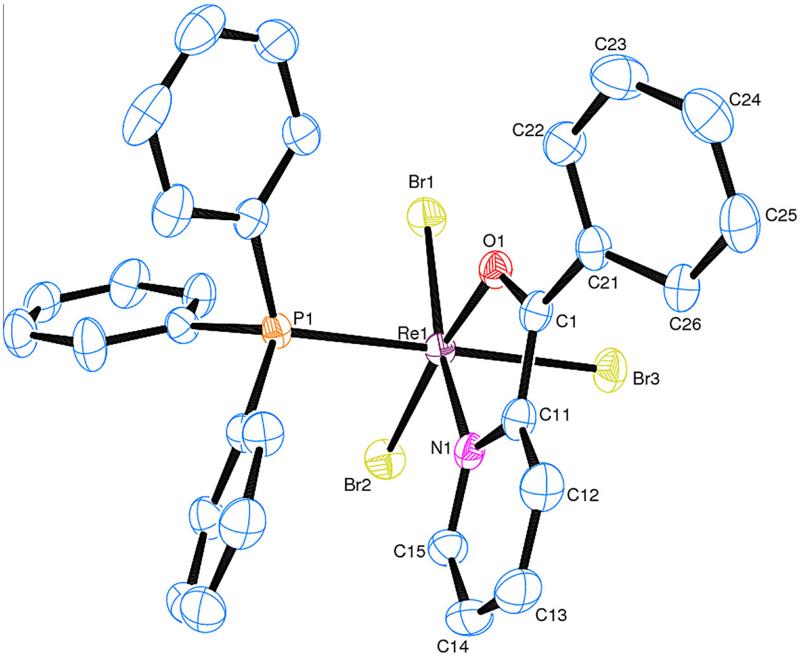

Fig. 4. ORTEP plot of **4** showing 40% probability displacement ellipsoids and the atom-numbering. Hydrogen atoms are omitted for clarity.

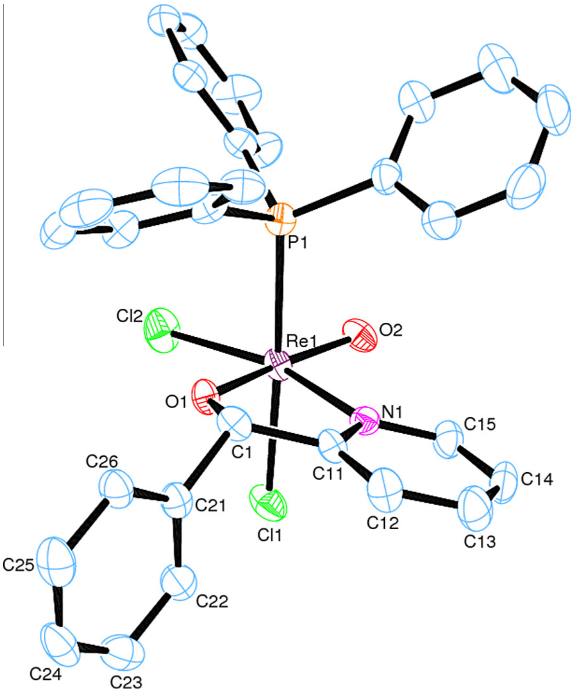

Fig. 5. ORTEP drawing of complex **5**.

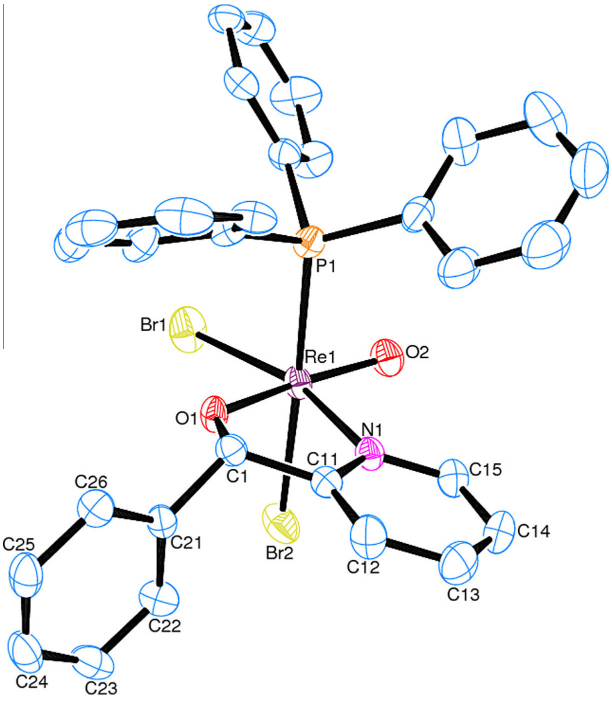

Fig. 6. ORTEP plot of complex **6**.

in the range 1610–1500 cm^{-1}. Two medium intensity bands at 329 and 318 cm^{-1} for the Re–Cl stretches in **5** indicate the presence of the two chlorides in non-equivalent *cis* positions. The lower value is assigned to the chloride coordinated in the position *trans* to the phosphine ligand. The metal-promoted transformation of the ketone group in zpy is supported by the broad singlet at 9.21 ppm in both the ^1H NMR spectra of **5** and **6**, attributed to the proton on the bridging carbon atom of the chelate. There are eight well separated signals for the nine aromatic protons of zpyH, with the signal of the ninth obscured by the peaks due to PPh_3. The electronic spectra in dichloromethane display ligand-to-metal charge transfer absorption bands at 345 and 365 nm in **5** and **6** respectively.

Perspective views of the asymmetric units of **5** and **6** are given in Figs. 5 and 6. The neutral complexes exhibit distorted octahedral geometries about the central rhenium(V) ion. The basal planes are defined by the phosphorus atom P(1), two halides *cis* to each other and the neutral pyridyl nitrogen N(1) of zpyH. The oxo group O(2) and the oxygen atom of zpyH O(1) are in *trans* axial positions. Distortion from an ideal rhenium-centered octahedron mainly results in a non-linear O(2)=Re–O(1) axis [162.6(1)° in **5** and 162.5(1)° in **6**], accomplished by Cl(1)–Re–P(1) and Cl(2)–Re–N(1) angles of 176.4(5)° and 164.01(1)° in **5** and Br(2)–Re–P(1) = 176.7(3)° and Br(1)–Re–N(1) = 164.0(1)° in **6**. The metal is lifted out of the mean equatorial plane formed by X_2PN by 0.240 and 0.241 Å in **5** and **6** respectively towards O(2), which is reflected in the non-orthogonal angles O(2)–Re–X(1) = 96.6(1)° in **5** and 105.3(9)° in **6**; O(2)–Re–X(2) = 105.6(1)° (**5**) and 96.2(1)° (**6**); and O(2)–Re–P(1) = 87.0(1)° (**5**) and 86.8(1)° (**6**). The Re=O(2) axis is inclined at 176.7° and 177.3° with respect to the equatorial planes in **5** and **6** respectively.

The Re=O(2) bond lengths of 1.700(3) and 1.686(3) Å are within the expected range with a phenolate *trans* to the oxo group [41]. The Re–O(1) bond lengths [1.919(3) Å (**5**); 1.920(3) Å (**6**)] are shorter than the usual length for a Re–O single bond [2.04 Å], which reflects the delocalization of the π-electron density from the oxo bond to the *trans* Re–O bond [42]. The Re–Cl(1) and Re–Br(2) bond distances are significantly longer than the Re–Cl(2) and Re–Br(1) bonds, due to the larger *trans* effect of the P compared to the pyridyl nitrogen N(1). The bite angle [O(1)–Re–N(2)] of the chelate is practically identical in both complexes (Table 2). The average C(1)–O(1) bond length [1.310(6) Å] is longer than that for a ketonic double bond.

The theoretical calculations show that the ground state of **5** and **6** are singlet and that the electronic configurations of rhenium are [core]6s(0.37)5d(5.48) and [core]6s(0.42)5d(5.53) respectively. The halides *cis* to phosphorus form a bond orbital with the rhenium, with the difference that the bromides share a larger portion of p electrons compared to the chlorides. In both cases, the halides *trans* to phosphorus behave differently to the halides in the *cis* positions, in that they form weaker bonds to rhenium than the *cis* ones. The second order perturbation theory analysis of the Fock matrix shows that the lone pair electrons of the halides *cis* to N(1) are delocalized on the Re–P(1) and Re–P(2) anti bond and Re lone pair and Rydberg star orbitals. The calculated Re–Cl(2), Re–Cl(1), Re–Br(1) and Re–Br(2) bond lengths are 2.386, 2.442, 2.589 and 2.654 Å respectively, which is consistent with the listed bond orders in Table 4 and the experimental data. In **5** and **6** the O(1) lone pair electrons are delocalized on the rhenium lone pair star, Re–O(2), Re-P(1), and Re–Cl (2) anti bond orbitals and on rhenium lone pair star, Re–O(2), Re–P(1), and Re–Br(1) anti bond orbitals respectively. In **5** the nitrogen lone pair electrons are delocalized on the rhenium lone pair star, Re–O(2), and Re–Cl(2) anti bond orbitals. Also, the N(1)–C(15) bond orbitals are delocalized on the Re–Cl(2) anti bond orbitals. In **6** nitrogen behaves similarly and instead of Re–Cl(2) anti bond orbital the electrons are delocalized on Re–Br(1) anti bond orbital. The phosphorus uses $sp^{2.8}$ hybrid orbitals to form a bond with rhenium in both complexes, and due to over-binding gains a positive natural charge. The Re=O bond orbitals in both complexes are composed of almost pure d and p electrons which are shared by the rhenium and oxygen respectively. The rhenium natural charge in **5** is more positive than in **6**, which is in good agreement with expectation.

3.5. *fac*-$[Re(CO)_3(zpy)Cl].C_7H_{8.}$ (**7**)

The title compound was synthesized from the reaction of $[Re(CO)_5Cl]$ with a twofold molar excess of zpy in toluene under a nitrogen atmosphere.

$$[Re(CO)_5Cl] + zpy \rightarrow fac\text{-}[Re(CO)_3(zpy)Cl] + 2CO$$

The complex is air-stable and soluble in DMF, DMSO and dichloromethane. The infrared spectrum in the solid state displays three strong absorption bands attributable to the carbonyl stretching frequencies of the *fac*-$[Re(CO)_3]^+$ core: a sharp intense band at 2021 cm^{-1} and two lower-energy bands at 1916 and 1857 cm^{-1}. This pattern corresponds to three CO units in a *facial* isomer arrangement [43]. A band at 1595 cm^{-1} is attributed to ν(C=O) of the ketone group and characteristic bands of C=C and C=N are observed in the range 1580–1550 cm^{-1}. The ^1H NMR of the complex consists of sharp, well-resolved peaks. The most informative aspect of the spectrum is the aromatic region that comprises of a single-proton doublet at 8.72 ppm (*H15*), a one-proton triplet at 8.08 (*H13*), a three-proton multiplet in the range 7.90–8.00 ppm, and two-proton triplets at 7.73 ppm (*H22*, *H26*) and 7.65 ppm (*H23*, *H25*). The UV–Vis spectrum in dichloromethane only shows a ligand-to-metal charge transfer absorption band at 475 nm.

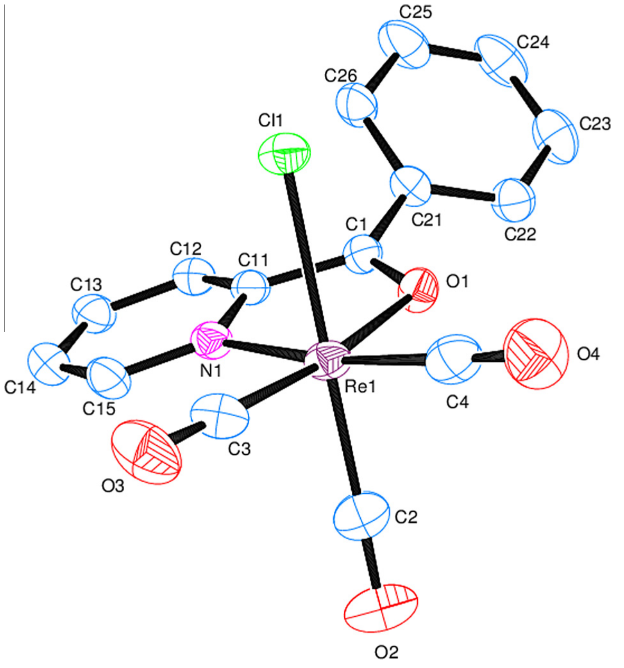

Fig. 7. ORTEP view of complex **7**. The toluene molecule is omitted for clarity.

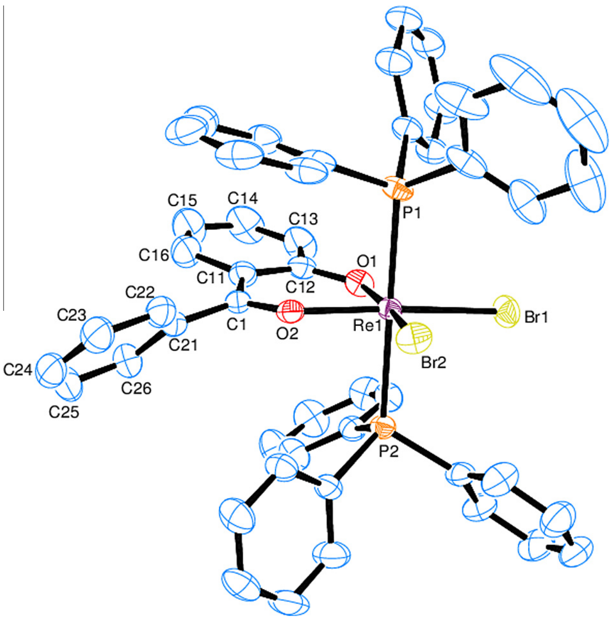

Fig. 8. ORTEP drawing of complex **8**.

The solvent-free complex **7** was synthesized previously by the reaction of equimolar quantities of [Re(CO)$_5$Cl] and zpy in toluene [36]. It crystallized in the monoclinic crystal system from dichloromethane.

Maroon crystals of **7**, suitable for X-ray crystallography, were obtained from the slow evaporation of the reaction mixture. A perspective view of the asymmetric unit is shown in (Fig. 7). It contains two molecules of [Re(CO)$_3$(zpy)Cl] and a toluene molecule of crystallization, and the crystal packing is governed by van der Waals contacts. No intermolecular hydrogen bonds exist and weak intramolecular hydrogen bonds are observed. The X-ray results show that the rhenium(I) complex contains the chemically robust *fac*-[Re(CO)$_3$]$^+$ core in a distorted octahedral geometry. The rhenium(I) is coordinated to three carbonyl donors in a *facial* orientation, to the pyridinyl nitrogen N(1), the ketonic oxygen O(2) and the chloride Cl(1). The Re–CO bond distances [average of 1.907(4) Å] (Table 2) fall in the range observed [1.900(2)–1.928(2) Å] for similar complexes [24,44]. The Re–N(1) bond length [2.162(3) Å] is slightly shorter than those observed in complexes **1** and **5**. The Re–O(1) bond length of 2.170(3) Å is remarkably longer than the Re–O bond distance in complex **5** [1.920(3) Å], proving that the oxygen O(1) is neutral. The C(1)–O(1) distance of 1.246(4) Å corresponds to that of a double bond, and the C(21)–C(1)–O(1) bond angle [119.3(3)°] is close to that for a sp^2-hybridized carbon atom. The ligand zpy therefore acts as a neutral bidentate N,O-donor ligand.

The distortion from octahedral ideality in the complex is mainly the result of the *trans* angles, with C(4)–Re–N(1) = 170.9(1)°, C(3)–Re–O(1) = 171.31(1)°, and C(2)–Re–Cl(1) = 176.2(1)°. These distortions are the result of the constraints imposed by the bidentate ligand zpy, which forms a five-membered [N(1)–Re–O(1) = 73.8(1)°] metalloring with the rhenium center. The steric repulsion between the chloride and the equatorially coordinated nitrogen atom [Cl(1)–Re–N(1) = 82.60(7)°] is larger than between the chloride and the axial oxygen [Cl(1)–Re–O(1) = 80.69(7)°]. The average C–Re–C bond angle of 89.3(2)° is close to orthogonality. The Re–N(1)–C(11) angle of 116.4(2)° is close to expectation for a sp^2 hybridized nitrogen. The dihedral angle between the pyridyl and phenyl rings of zpy is 40.1°.

The theoretical calculations show that the ground state of **7** is singlet and that the electronic configuration of rhenium is [core]6s(0.42)5d(6.58). The CO ligands form the strongest bonds to the rhenium. The carbon atoms use sp$^{\sim 0.6}$ hybrid or pure p electrons to bind to the rhenium. The rhenium uses pure d electrons and the larger polarization coefficient (~0.91) belongs to the transition metal. The Re–Cl (1), Re–N(1) and Re–O(1) bonds are too weak and the Cl(1), N(1) and O(1) lone pairs are almost delocalized on Re–C(2), Re–C(4), and Re–C(3) anti bond orbitals respectively. The calculated Re–O(1) bond distance is remarkably larger than usual Re–O bonds which is consistent with its small bond order. The carbon atoms that are bound to electronegative oxygen atoms and share their electrons with the rhenium gain positive charges. The natural charges of the other donor atoms are negative, and thereby creating no charge on the rhenium.

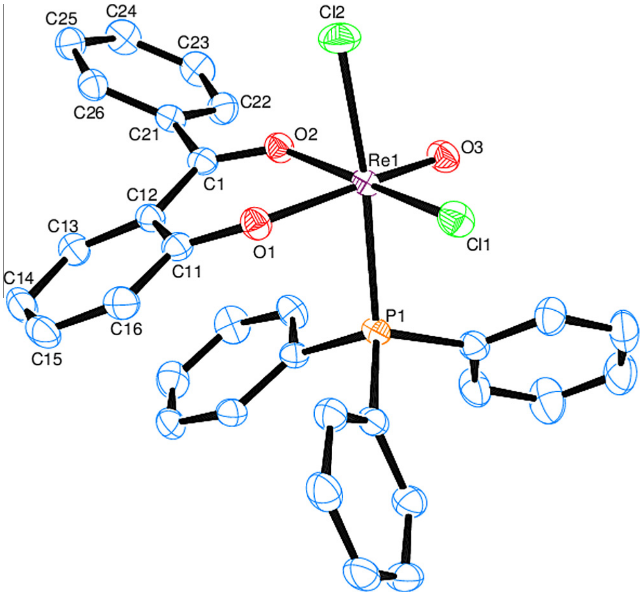

Fig. 9. ORTEP drawing of complex **9** showing the atom-numbering.

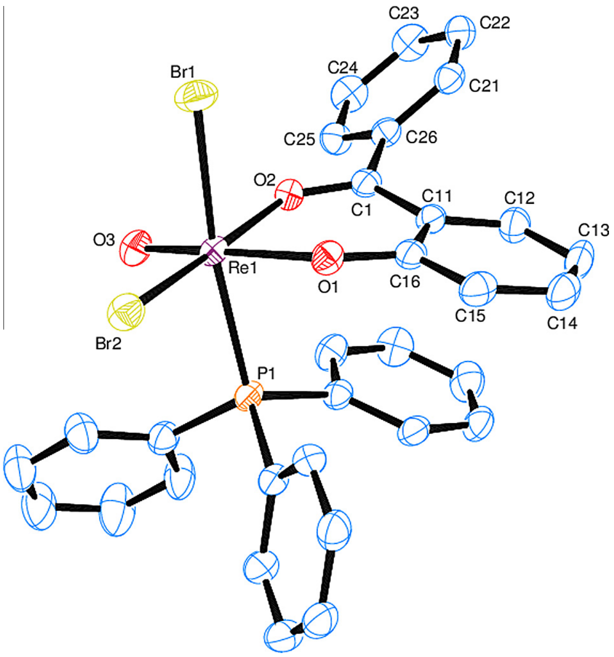

Fig. 10. ORTEP plot of complex **10** showing the atom-numbering.

3.6. *cis*-[ReBr$_2$(bp)(PPh$_3$)$_2$] (**8**)

The rhenium(III) compound **8** was prepared in good yield by the reaction of *trans*-[ReOBr$_3$(PPh$_3$)$_2$] with Hbp in a 1:2 M ratio in methanol. The surprising aspect of this reaction is the reduction of the oxorhenium(V) center to rhenium(III), especially in the presence of air. The reduction of the metal normally occurs by abstraction of the oxo group by PPh$_3$ to form OPPh$_3$. The complex has a low solubility in polar solvents such as acetone and acetonitrile and is stable for months in the solid state, and is a non-electrolyte in DMF. The infrared spectrum exhibits no absorption in the 890–1020 cm^{-1} region that could be attributable to ν(Re^{V}=O). The single peaks in the IR spectrum at 1630 and 436 cm^{-1} are assigned to ν(C=O) and ν(Re–O) respectively, which illustrate the coordination behavior of the bp chelate in the complex. The ^{1}H NMR spectrum consists of poorly-resolved broad peaks, showing paramagnetic shifts and line broadening of the signals and could not be used constructively in deducing the structure of the complex.

The crystal structure of the complex (Fig. 8) reveals that the rhenium atom is at the center of a distorted octahedron. The basal plane is defined by the phenolate and ketonic oxygens O(1) and O(2) and two bromine atoms Br(1) and Br(2). The two phosphorus atoms are in *trans* axial positions. The P(1)–Re–P(2) axis [179.2(3)°] is linear, with the other *trans* angles Br(1)–Re–O(2) = 172.4(6)° and Br(2)–Re–O(1) = 171.7(6)° deviating from linearity (Table 2). The metal is shifted out of the mean O_2Br_2 equatorial plane formed by 0.169 Å towards P(2), with the angles P(2)–Re–Br(1) = 86.6(2)°, P(2)–Re–O(1) = 90.3(6)°, P(2)–Re–O(2) = 88.9(6)° and P(2)–Re–Br(2) = 92.4(2)°. The bite angle of the bp chelate is O(1)–Re–O(2) = 85.5(8)°.

The Re–P lengths of 2.463(6) and 2.475(6) Å agree well with the average of 2.470 Å found in other rhenium(III) complexes containing two *trans* triphenylphosphine ligands [45,46]. The Re–O(1) bond length of 1.992(2) Å is typical of a single rhenium-phenolate bonds and falls in the range found for this type of bond in similar complexes [47]. The O(2)–C(1) bond is double [1.283(3) Å], and the bonding in the molecule is complemented by a O(2)–H···C(66) hydrogen bond.

The theoretical calculations show that the ground state of **8** is triplet and that the electronic configuration of rhenium is [core]6s(0.43)5d(6.00). The bromine ligands form slightly stronger bonds to rhenium than the other donor atoms. The data in Table 4 show that the bond orders for Re–O(1) and Re–O(2) are 0.35 and 0.23 respectively. The C(11)–C(16) phenyl ring resonates with bond c12–O(1); however, there is no such a resonance for O(2). As a result, the bond orders for Re–O(1) and Re–O(2) are different. In the Re–P(1) and Re–P(2) bonds the rhenium and phosphorus atoms use $sd^{1.29}$, $sp^{2.38}$ and $sd^{1.53}$, $sp^{2.39}$ hybrid electrons respectively, and the phosphorus atoms have a larger polarization coefficient (~0.81) in both bonds. The O(2), O(1), P(1) and P(2) lone pair electrons are delocalized on Re–Br(1), Re–Br(2), Re–P(2) and Re–P(1) anti bond orbitals respectively. The phosphorus atoms, due to over-binding, gain positive charges with negative charges aggregating on the other donor atoms. Overall, the rhenium natural charge is not as positive as in the complexes with less than two phosphorus atoms.

3.7. *cis-[ReOX$_2$(bp)(PPh$_3$)]* (*9* and *10*)

The reactions of *trans*-[$ReOX_3(PPh_3)_2$] (X = Cl, Br) with a twofold molar excess of the ligand Hbp in acetonitrile under reflux gave the green complexes [$ReOX_2$(bp)(PPh_3)] [X = Cl(**9**), Br(**10**)] as products. None of these complexes could be isolated with an equimolar ratio of reactants, even in the presence of triethylamine. Both complexes are diamagnetic (formally d^2) and have low solubilities in polar solvents like DMSO, acetone and chloroform. In the infrared spectra the asymmetric Re=O stretching frequencies [948 cm^{-1} (**9**), 974 cm^{-1} (**10**)] appear as sharp strong bands and fall in the region of 945–965 cm^{-1} that is normally observed for neutral six-coordinate monooxorhenium(V) complexes with an anionic phenolate oxygen atom coordinated *trans* to the Re=O moiety [40,48,49]. Deprotonation of the phenolic OH groups in each complex is supported by the absence of a band in the 3200–3500 cm^{-1} region. The ^1H NMR spectrum of **9** consists of a two-proton doublet at 7.69 ppm, an eighteen-proton multiplet in the region 7.51–7.64 ppm, and a four-proton multiplet in the region 6.92–7.01 ppm. The spectrum of **10** integrates for twenty-four protons in the aromatic region, and the overlap of the signals of the chelate with those of PPh_3 makes assignments difficult.

The structures of **9** (Fig. 9) and **10** (Fig. 10) consist of discrete, monomeric and neutral oxorhenium complexes packed with no intermolecular contacts shorter than the Van der Waals radii sum. The coordination geometry around the rhenium is highly distorted octahedral; the ketonic oxygen from the bidentate uninegative ligand O(2) lie on the equatorial plane, along with the two *cis* halides X(1) and X(2) and phosphorus P(1) atoms, with the phenolate O(2) *trans* to the O(1) oxo atom. In the two complexes the O(1)–Re–O(3) axis is non-linear [166.0(6)° and 166.1(8)° in **9** and **10** respectively], and the rhenium atom is displaced from the mean equatorial plane by 0.073(1) and 0.12(1) Å in **9** and **10** respectively towards the oxo oxygen atom. The interligand angles in the equatorial planes depart considerably from the ideal 90° [from 88.3(6)° to 98.9(5)° (**9**) and from 84.2° to 98.9(5)° (**10**)].

The Re=O(3) distances of 1.689(1) Å (in **9**) and 1.675(2) Å (in **10**) compare favorably with those reported previously [50–56]. As expected, the Re–O(1) bond lengths, *trans* to the oxo oxygen O(3), are significantly shorter than the equatorial Re–O(2) bond lengths [*e.g.* 1.966(1) versus 2.089(1) Å in **9**; 1.967(2) versus 2.088(2) Å in **10**]. The C(1)–O(2) bond length [1.262(2) Å in **9**; 1.262(3) Å in **10**] shows this to be a double bond, with the C(11)–O(1) and C(16)–O(1) bonds single [1.336(2) Å in **9**; 1.336(3) Å in **10**]. The O(2)–C(11)–C(12) angle in **9** [122.0(2)°] and O(2)–C(1)–C(11) bond angle in **10** [123.0(2)°] show that the C(1) atom is *sp^2*-hybridized, and that no nucleophilic attack has occurred. The Re–X(2) bond distance in **9** is significantly longer than the Re–X(1) bond length, due to the larger *trans* effect of the phosphorus atom compared to the ketonic oxygen O(2) (Table 2). The latter is also observed in **10**. The bite angle [O(1)–Re–O(2) of 81.0(7)° (**9**) and 80.9(7)° (**10**)] of the bp ligand is practically identical, and they are about 4.5° smaller than in complex **8**.

The theoretical calculations show that the ground states of **9** and **10** are singlet and the rhenium electronic configurations are [core]6s(0.37)5d(5.44) and [core]6s(0.41)5d(5.50) respectively. The electronegative chlorine ligands have a larger polarization coefficient factor in the Re–halide bond orbitals than the comparative bromines, and using fewer p electrons. The Re–O(3) bond orders of 1.60 and 1.56 in **9** and **10** are in agreement with the sharp strong bands in the IR spectra. Also, the calculated O(1)–Re–O(3) angles of 166.1° and 166.0° for **9** and **10** are in exact agreement with the experimental data. The calculations show that the Re–Cl(2) bond distance in **9** is longer than the Re–Cl(1) bond length, and the Re–Br(1) bond distance in **10** is longer than the Re–Br(2) bond length. In the Re–P(1) bond orbital the rhenium and phosphorus atoms use $sp^{1.91}d^{1.96}$ and $sp^{2.91}$ hybrid electrons respectively, and the large polarization coefficient (~0.91) of the phosphorus shows that electrons are effectively localized on this ligand. In **9**, the O(1) and O(2) lone pair electrons are delocalized on Re–O(3) and Re–Cl (1) anti bond orbitals respectively, and in **10** the P(1), O(1) and O(2) lone pair electrons are delocalized on the Re-Br(1), Re–O(3) and Re–Br(2) anti bond orbitals respectively. The presence of more electronegative ligands in **9** compared to **10** enables the rhenium to gain a larger positive charge.

4. Conclusion

The reaction of dpk with [$Re(CO)_5Cl$] in methanol led to the nucleophilic attack of methanol on the bridging ketonic group, to produce the coordinated monoanionic tridentate ligand dpk·OCH_3 in the complex *fac*-[$Re(CO)_3$(dpk·OCH_3)] (**1**). In the reaction of dpk with *trans*-[$ReOBr_3(PPh_3)_2$] in acetone, the ketonic group is attacked by water to yield the coordinated monoanionic tridentate ligand in the complex [$ReOBr_2$(dpk·OH)].

The reaction of zpy with *trans*-[$ReOX_3(PPh_3)_2$] in acetonitrile led to the reduction of the metal to +III, with no nucleophilic attack on the ketonic group in the complexes [$ReOX_2$(zpy)(PPh_3)]. However, with methanol as solvent, no reduction of the metal occurred, but again the zpy had undergone nucleophilic attack by water, and not methanol as observed in complex **1**, in the complexes [$ReOX_2$(zpy·OH)(PPh_3)]. With [$Re(CO)_5Cl$] in toluene under nitrogen, no attack happened on zpy and the complex *fac*-[$Re(CO)_3Cl$(zpy)] was isolated.

With Hbp, the rhenium(III) complex *cis*-[$ReBr_2$(bp)$(PPh_3)_2$] was formed in the reaction of *trans*-[$ReOBr_3(PPh_3)_2$] in methanol. Changing the solvent to acetonitrile, the complexes [Re^VOX_2(bp)(PPh_3)] were isolated. This is in contrast to what was observed with zpy as ligand.

From an atomistic point of view the CO groups and the oxo oxygen ligands bind stronger to the rhenium rather than the other ligands. The phosphorus and carbon atoms bonded to the rhenium are the only donor atoms to gain positive charges in all the complexes, which are caused by the over-bonding to four atoms and connecting to electronegative oxygen and the rhenium respectively. The bigger bromine ligands use a larger portion of p electrons than the smaller chlorine to bind to the rhenium. In the complexes where there is not any significant local bond orbital between donor atoms and rhenium, the donor atoms' lone pair electrons are usually delocalized on the front anti bond orbitals.

Acknowledgments

We would like to thank the Theoretical and High Performance Computational Research Center of Razi University for providing the DFT calculation facilities. TIAG is grateful to the Nelson Mandela Metropolitan University for financial support.

Appendix A. Supplementary data

CCDC 935177, 935283, 936087, 935347, 935938, 935933, 936165, 935907, 935891, 935546 contains the supplementary crystallographic data for compounds **1**–**10**, respectively. These data can be obtained free of charge via http://www.ccdc.cam.ac.uk/conts/retrieving.html, or from the Cambridge Crystallographic Data Centre, 12 Union Road, Cambridge CB2 1EZ, UK; fax: (+44) 1223-336-033; or e-mail: deposit@ccdc.cam.ac.uk.

References

[1] (a) T.I.A. Gerber, H.J. Kemp, J.G.H. du Preez, G. Bandoli, J. Coord. Chem. 28 (1993) 329;
(b) M. Bakir, Acta Crystallogr., Sect. C 58 (2002) m74;
(c) C. Pejo, H. Pardo, A. Mombrú, M.F. Cerdá, J.S. Gancheff, R. Chiozzone, R. González, Inorg. Chim. Acta 376 (2011) 105.

[2] J.G. Malecki, R. Kruszynki, Polyhedron 26 (2007) 2686.

[3] D.L. Reger, J.R. Gardinier, M.D. Smith, P.J. Pellechia, Inorg. Chem. 42 (2003) 482.

[4] Y. Fuchita, H. Ieta, Y. Tsunemune, J. Kinoshita-Nagaoka, H. Kawano, J. Chem. Soc., Dalton Trans. (1998) 791.

[5] (a) B. Machura, J. Mroziński, R. Kruszynski, J. Kusz, Polyhedron 28 (2009) 2821;
(b) B. Machura, M. Wolff, A. Świtlicka, R. Kruszynski, J. Kusz, Inorg. Chem. Commun. 12 (2009) 789.

[6] M. Bakir, J.A.M. McKenzie, J. Chem. Soc., Dalton Trans. (1997) 3571.

[7] (a) B. Machura, J. Mroziński, J. Kusz, Inorg. Chem. Commun. 13 (2010) 231;
(b) B. Machura, J. Miłek, R. Kruszynski, J. Kusz, J. Mroziński, Polyhedron 27 (2008) 1262.

[8] N.P. Johnson, C.J.L. Lock, G. Wilkinson, Inorg. Synth. 9 (1967) 145.

[9] G.M. Sheldrick, SADABS, University of Göttingen, Germany, 1996.

[10] G.M. Sheldrick, Acta Crystallogr., Sect. A 64 (2008) 112.

[11] A.A. Granovsky, Firefly, version 8.0.0. <http://classic.chem.msu.su/gran/firefly/index.html>.

[12] E.D. Glendening, J.K. Badenhoop, A.E. Reed, J.E. Carpenter, J.A. Bohmann, C.M. Morales, F. Weinhold, NBO 5.0, Theoretical Chemistry Institute, University of Wisconsin, Madison, 2001.

[13] A.D. Becke, J. Chem. Phys. 98 (1993) 5648.

[14] P.J. Stephens, F.J. Devlin, C.F. Chabalowski, M.J. Frisch, J. Phys. Chem. 98 (1994) 11623.

[15] K.L. Schuchardt, B.T. Didier, T. Elsethagen, L. Sun, V. Gurumoorthi, J. Chase, J. Li, T.L. Windus, J. Chem. Inf. Model. 47 (2007) 1045.

[16] V. Yeguas, P. Campomanes, R. López, Dalton Trans. 39 (2010) 874.

[17] F. Taherkhani, F.R. Negreiros, G. Parsafar, A. Fortunelli, Chem. Phys. Lett. 498 (2010) 312.

[18] F.R. Negreiros, F. Taherkhani, G. Parsafar, A. Caro, A. Fortunelli, J. Chem. Phys. 137 (2012) 194302.

[19] M. Nahali, F. Gobal, R. Arab, Mol. Phys. 109 (2011) 1797.

[20] A. Arab, F. Gobal, N. Nahali, M. Nahali, J. Cluster Sci. 24 (2013) 273.

[21] C.H. Chang, A.J. Boone, J.B. Rodney, G.J. Nigel, Inorg. Chem. 43 (2004) 458.

[22] V. Tangoulis, C.P. Raptopoulou, S. Paschalidou, A.E. Tsohos, E.G. Balkalbassis, A. Terzis, S.P. Perlepes, Inorg. Chem. 36 (1977) 5270.

[23] (a) P. Mayer, K.C. Potgieter, T.I.A. Gerber, Polyhedron 29 (2010) 1423;
(b) M. Bakir, J.A.M. McKenzie, J. Electroanal. Chem. 425 (1997) 621.

[24] L. Wei, S.R. Banerjee, M.K. Levadala, J. Babich, J. Zubieta, Inorg. Chim. Acta 357 (2004) 1499.

[25] L. Maria, C. Moura, A. Paulo, I.C. Santos, J. Organomet. Chem. 691 (2006) 4773.

[26] Z.R. Tshentu, T.I.A. Gerber, R. Walmsley, P. Mayer, Polyhedron 27 (2008) 406.

[27] T.I.A. Gerber, P. Mayer, Z.R. Tshentu, J. Coord. Chem. 58 (2004) 1271.

[28] A. Abrahams, T.I.A. Gerber, P. Mayer, J. Coord. Chem. 58 (2005) 1387.

[29] G. Bandoli, A. Dolmella, T.I.A. Gerber, D. Mpinda, J. Perils, J.G.H. du Preez, J. Coord. Chem. 55 (2000) 823.

[30] U. Mazzi, E. Roncari, R. Rossi, V. Bertolasi, O. Traverso, L. Magon, Transition Met. Chem. 5 (1980) 289.

[31] F.A. Cotton, S.J. Lippard, Inorg. Chem. 4 (1965) 1621.

[32] T.I.A. Gerber, A. Abrahams, C. Imrie, P. Mayer, J. Coord. Chem. 57 (2004) 1339.

[33] P. Ghosh, A. Pramanik, N. Bag, A. Chakravorty, J. Chem. Soc., Dalton Trans. (1992) 1883.

[34] E. Marchesi, A. Marchi, L. Marvelli, M. Peruzzini, M. Brugnati, V. Bertolasi, Inorg. Chim. Acta 358 (2005) 352.

[35] B. Machura, R. Kruszynski, M. Jaworska, P. Lodowoski, Polyhedron 24 (2005) 701.

[36] M. Siervert, R. Dienelt, H. Bock, Acta Crystallogr., Sect. C 54 (1998) 674.

[37] B. Machura, R. Kruszynski, J. Organomet. Chem. 692 (2007) 4161.

[38] D. Orth, J. Barrerra, M. Sabat, W.D. Harman, Inorg. Chem. 33 (1994) 3026.

[39] S.R. Fletcher, A.C. Skapski, J. Chem. Soc., Dalton Trans. (1972) 1073.

[40] B. Machura, R. Kruszynski, J. Mroziński, J. Kusz, Polyhedron 27 (2008) 1739.

[41] A.L. Wilds, Org. React. (1944) 2.

[42] T.I.A. Gerber, D. Luzipo, P. Mayer, Inorg. Chim. Acta 357 (2004) 429.

[43] X. Chen, F.J. Femina, J.W. Babich, J. Zubieta, Inorg. Chim. Acta 308 (2002) 80. and references therein.

[44] T.I.A. Gerber, H.J. Kemp, J.G.H. du Preez, G. Bandoli, A. Dolmella, Inorg. Chim. Acta 202 (1992) 191.

[45] J. Granifo, Polyhedron 1061 (1999) 18.

[46] B. Machura, A. Switlicka, I. Nawrot, K. Michalik, Inorg. Chem. Commun. 13 (2010) 1317.

[47] C. Melian, C. Kremer, K. Suescun, A. Mombru, R. Mariezcurrena, E. Kremer, Inorg. Chim. Acta 306 (2000) 70.

[48] I.D. Brown, C.J.L. Lock, C. Wan, Can. J. Chem. 52 (1974) 1704.

[49] B. Machura, M. Wolff, J. Mrozinski, R. Kruszynski, J. Kusz, Polyhedron 28 (2009) 2377.

[50] H. Pietzch, H. Spies, P. Leibnitz, G. Reck, Polyhedron 1849 (1995) 14.

[51] U. Witten, J. Strahle, U. Abram, Z. Anorg. Allg. Chem. 621 (1995) 1338.

[52] T.I.A. Gerber, D. Luzipo, P. Mayer, J. Coord. Chem. 56 (2003) 1549.

[53] T.I.A. Gerber, D. Luzipo, P. Mayer, J. Coord. Chem. 58 (2004) 1505.

[54] W.A. Herrmann, M.U. Rauch, G.R.J. Artus, Inorg. Chem. 1996 (1988) 35.

[55] H.J. Banbery, F. McQuillan, T.A. Hamor, C.J. Jones, J.A. McCleverty, J. Chem. Soc., Dalton Trans. (1989) 1405.

[56] A. Abrahams, G. Bandoli, S. Gatto, T.I.A. Gerber, J.G.H. du Preez, J. Coord. Chem. 42 (1997) 303.